



7N-26
193729
P-52

TECHNICAL NOTE

D-270

EFFECT OF HARDNESS AND OTHER MECHANICAL PROPERTIES
ON ROLLING-CONTACT FATIGUE LIFE OF FOUR
HIGH-TEMPERATURE BEARING STEELS

By Thomas L. Carter, Erwin V. Zaretsky
and William J. Anderson

Lewis Research Center
Cleveland, Ohio

NATIONAL AERONAUTICS AND SPACE ADMINISTRATION
WASHINGTON

March 1960

(NASA-TN-D-270) EFFECT OF HARDNESS AND
OTHER MECHANICAL PROPERTIES OF
ROLLING-CONTACT FATIGUE LIFE OF FOUR
HIGH-TEMPERATURE BEARING STEELS (NASA)
52 F

N89-70480

Unclas
00/26 0198729

NATIONAL AERONAUTICS AND SPACE ADMINISTRATION

TECHNICAL NOTE D-270

EFFECT OF HARDNESS AND OTHER MECHANICAL PROPERTIES ON
ROLLING-CONTACT FATIGUE LIFE OF FOUR
HIGH-TEMPERATURE BEARING STEELS

By Thomas L. Carter, Erwin V. Zaretsky
and William J. Anderson

SUMMARY

The fatigue spin rig and the five-ball tester were used to determine the rolling-contact fatigue life at room temperature of groups of AISI M-1, AISI M-50, Halmo, and WB-49 alloy steel balls tempered to various hardness levels. Nominal test conditions included 800,000-psi maximum theoretical (Hertz) compressive stress and a synthetic-diester-base lubricant. The fatigue-life results were compared with: material hardness, resistance to plastic deformation in rolling contact, and previously published tensile and compressive strength data for these same heats of material. The following results were obtained.

Rolling-contact fatigue life and load-carrying capacity of each of the four alloy compositions studied increased continuously as material hardness increased. The improvement in load capacity was in the order of 30 to 100 percent over the hardness range tested. No maximum fatigue life or load capacity at intermediate hardness values was observed.

The fatigue results obtained in this investigation did not correlate with previously published tension and compression strength data for bar specimens from the same heats of material, which showed an apparent optimum strength at intermediate hardness values. This investigation, however, showed that resistance to permanent plastic deformation of specimens in rolling contact increased continuously with increasing hardness. These conflicting trends of resistance to plastic deformation as measured with contacting spheres and as measured by elastic limit and yield strength of bar specimens indicate that very hard bar specimens may be susceptible to significant overstressing because of eccentric loading.

Only minor differences in metallographic structure were observed for the different hardness levels of each alloy considered. The softer balls tended to have more and larger fine (precipitated) carbides and greater definition of tempered martensite. Percent retained austenite decreased with lower hardness (higher tempering temperature).

INTRODUCTION

As a part of the overall attempt to improve the operating life of rolling-contact bearings, much effort is being spent on relating the effect of various material properties to the fatigue life of the bearing elements. Any correlation between an easily measured property of bearing materials and rolling-contact fatigue life may be very helpful in screening potential bearing materials.

Elastic limit and hardness are, respectively, measures of the minimum stress required for, and the resistance to, permanent deformation of a material. Although material fatigue can occur at stress levels considerably below that associated with plastic deformation, yield strength and resistance to impression (hardness) are basic measures of material strength and hence offer promise of correlation with fatigue life. Although the rate of strain used in determining both properties is low compared with that encountered in high-speed rolling-contact bearings, the rate used in determining hardness is somewhat higher than that of the elastic-limit determination. Furthermore, the stress pattern generated by the contact of the hardness indenter is more similar to that of bodies in rolling contact than is the stress pattern in a tension or compression test specimen. For these reasons, hardness may be a measurable material property that correlates with fatigue.

It is well known that mechanical strength increases with increasing material hardness (ref. 1). Single ball tests have shown an increase in life with higher hardness (ref. 2). Furthermore, unpublished full-scale bearing data show an improvement in rolling-contact fatigue life with increasing material hardness. These data did not include, however, the ultimate hardness obtainable.

The work of Muir, Averbach, and Cohen (ref. 3) has shown, for the materials they tested, that mechanical-strength properties increase with higher hardness to a maximum and then decrease at very high hardness values. This suggests that maximum rolling-contact fatigue life for a given alloy composition may also be obtained at a hardness level below the maximum obtainable for that material.

The object of the research described herein was to investigate the effect of material hardness on the rolling-contact fatigue life of several tool steels and to compare fatigue-life results with other material properties associated with hardness. These material properties include: resistance to plastic deformation and wear, percent retained austenite, elastic limit, yield strength, and ultimate strength in both tension and compression. All experimental results for a given alloy composition were obtained from the same heat of material.

APPARATUS

The rolling-contact fatigue spin rig (figs. 1(a) and (b)) and the five-ball fatigue tester (figs. 1(c) and (d)) were used in these tests.

Fatigue Spin Rig

The fatigue spin rig is described in detail in reference 4. Essentially it consists of two balls driven at high speed on the inner surface of a race cylinder by an air jet (fig. 1(b)). Loading is applied by centrifugal force. Instrumentation provides for speed control and automatic failure detection and shutdown..

Five-Ball Fatigue Tester

The five-ball fatigue tester essentially consists of a driven test ball pyramided upon four lower balls positioned by a separator and free to rotate in an angular-contact raceway. Specimen loading and drive is supplied through a vertical shaft. By varying the pitch diameter of the four lower balls, bearing contact angle θ (fig. 1(d)) may be controlled. By utilization of a failure-detection and shutdown system, long-term unmonitored tests were made possible.

Lubrication was accomplished by introducing droplets of synthetic diester fluid lubricant, Mil-L-7808, into an airstream directed at the test specimen. Lubricant flow rate was controlled by adjusting the pressure upstream of a long capillary tube; the pressure drop through the capillary was sufficient to give excellent control for the small flow rates required.

The specimen was loaded by dead weights acting on the spindle through a load arm. Contact load was a function of the applied load and the contact angle. For every one revolution the spindle made, the test specimen was stressed three times. Analysis of this is shown in appendix A.

The bearing housing assembly was supported by rods held in flexible rubber mounts (fig. 1(c)). Positioning of the rods and rubber mounts provides for alinement of the raceway and four lower balls with the upper test ball and drive shaft. Minor misalignments are absorbed by the flexible rubber mounts. Vertical oscillations of the drive shaft created by rig vibration are dampened by the rubber mounts. Such vibrations, if not dampened, will increase the stress level of the ball specimen, thus influencing fatigue-life results.

E-524

CB-1 back

Choice of test-specimen rotative speed was provided through step pulleys driven by an electric motor. A magnetic pickup feeding an electronic counter provided for precise speed measurement.

Ambient temperature was measured with a thermocouple in contact with the raceway containing the freely rotating lower balls. Temperature calibrations show that the temperature recorded by the thermocouple was within 1 percent of the test-specimen ambient temperature.

Test Specimens

Ball specimens of 9/16-inch diameter were made from AISI M-1, AISI M-50, and Halm tool steels having the nominal chemical compositions shown in table I. These specimens were fabricated from the same heats of material as were used to fabricate bar specimens used by another investigator to establish tension and compression strengths for these alloys (refs. 5 and 6). This identity of material origin makes possible the direct comparisons of ball and bar tests that are discussed later. Ball specimens of 1/2-inch diameter were made from WB-49 tool steel having the nominal composition shown in table I.

Groups of balls from each of these four materials were heat-treated to give the range of hardness, in three or four increments, shown in table II. For each alloy composition the tempering temperature was the only variable in specimen preparation, and thus the controlled variable was material hardness.

Race cylinders for the spin rig were made from the same heats of AISI M-1, AISI M-50, and Halm as the ball specimens. All cylinders from the same alloy received the same fabrication and heat treatment so that they had the same hardness (Rockwell C-62 to 63). Thus, cylinders run with the varying hardness ball groups of a given alloy were nominally identical.

PROCEDURE

The support balls for the five-ball tester were grouped in sets of four having diameters matched within less than ten-millionths of an inch to insure even loading of the test specimen at all four contact points.

Before assembly, all test-section components were flushed and scrubbed with absolute ethyl alcohol and wiped dry with clean cheesecloth. Before running, the test specimens were weighed, measured, and examined for imperfections at a magnification of 60. Before a test was begun, the specimens and all contacting surfaces were coated with test lubricant.

E-524

After completion of a test in the fatigue spin rig, the race track was examined visually for imperfections. If the track on the spin rig cylinder was failed, the tests would be resumed on a new track in the same cylinder. Likewise, in the five-ball tester the support balls were examined. All four support balls were replaced if a fatigue spall or mechanical damage was found in any one of them.

Speed and oil flow were monitored and recorded at regular intervals. Tests were run at an ambient temperature of about 75° F in the spin rig and about 150° F in the five-ball fatigue tester. The higher temperature in the five-ball fatigue tester was caused by frictional heating.

The stress developed in the contact area under a particular load was calculated by using the modified Hertz formula given in reference 7.

Total running time for each specimen was recorded and converted into total stress cycles. Failure data were plotted on Weibull paper, which is a plot of the log log of the reciprocal of the probability of survival against the log of the stress cycles to failure. A more detailed description is given in reference 8. From this plot, the number of stress cycles necessary to fail any given portion of a specimen group may be determined. The 10-percent life, which is the number of stress cycles within which one-tenth of the specimens can be expected to fail, is determined by this method and is used as a value for fatigue life.

Measurement of Deformation and Wear

Deformation traces of the test specimens were made on a Talyrond Contour Tracer. By use of this machine the effect of the number of stress cycles and test conditions on permanent deformation was studied. Deformation produced on surfaces in rolling contact takes three basic forms: (1) elastic deformation due to contact stresses, (2) plastic deformation due to excessive stresses and repeated loading, and (3) wear of the contacting surfaces due to relative sliding. The first shows no effect on the specimen profile upon removal of the load. The latter two result in the permanent alteration of the ball. Figure 2(a) is a diagram of the transverse section of a ball surface showing this condition. A diagram of a Talyrond trace of this transverse section, which magnifies deviations from a true sphere, would appear as shown in figure 2(b).

The profile in figures 2(a) and (b) shows that the material has been added to the surface immediately adjacent to the running track. The region of increased volume extends approximately one track width on either side. If wear did not take place, the volume of material added to the region adjacent to the track should equal the volume of material displaced from the track itself since steels are essentially incompressible. However, this is not the case. The volume lost in figure 2 is much greater than the volume gained. The difference represents material removed by wear.

It should be noted that the radial distance on a Talyrond trace such as shown schematically in figure 2(b) is of a much higher magnification (X2000) than the circumferential distance (X30). From figure 2(b) it can be seen that, due to the convergence of the transverse distance in areas closer to the center, the areas of deformation and wear cannot be measured directly. To accurately measure the areas, the Talyrond trace is projected at X5 magnification and drawn on polar grid paper. The converging transverse distances are then adjusted mathematically to compensate for the unequal magnification. The areas of deformation and of deformation plus wear on the trace were measured by use of a planimeter, and their volumes were calculated. The wear volume is the difference between these two volumes.

E-524

Retained Austenite Determinations

The percent by volume of retained austenite in the metallographic structure was determined by X-ray diffraction techniques for specimens from each of the heat treatments of the four alloys studied. A series of calibration specimens with a known percent austenite was prepared by inserting austenitic stainless-steel wires in a cross section of low-carbon (ferritic) steel. The intensity of a diffraction line characteristic of austenite was measured for the known specimens, and a calibration curve of percent austenite against diffraction-line intensity was plotted. This calibration was used to determine the percent retained austenite given in table II in the metallographic structure of the balls receiving the various heat treatments.

RESULTS AND DISCUSSION

Rolling-Contact Fatigue Studies

Groups of 9/16-inch-diameter AISI M-1, AISI M-50, and Halmo steel balls having material hardness as the controlled variable were tested in the fatigue spin rig. Standard test conditions were room temperature (no heat added), a synthetic diester lubricant, and a ball loading that produced a maximum theoretical (Hertz) compressive stress of 800,000 psi per square inch. WB-49 steel balls of 1/2-inch diameter having hardness as the controlled variable were tested in the five-ball tester under the same standard test conditions. Specimen groups from each of the four alloys were heat-treated according to the schedule of table II to give increments of material hardness.

AISI M-1 balls. - Rolling-contact fatigue-life results for Rockwell C 62, 64.5, and 66 AISI M-1 specimen groups are given as Weibull plots in figures 3(a) to (c). Figure 3(d) is a summary figure showing 10-percent failure lives of 97×10^6 , 570×10^6 , and 695×10^6 stress cycles, respectively.

AISI M-50 balls. - Results for Rockwell C 60, 60.5, 62, and 63 AISI M-50 balls are given as Weibull plots in figures 4(a) to (d). A summary of these results in figure 4(e) shows 10-percent failure lives of 65×10^6 , 116×10^6 , 176×10^6 , and 182×10^6 stress cycles, respectively.

Halmo balls. - Because of speed limitations of the test apparatus, the test stress for this alloy was reduced from the standard stress of 800,000 psi to 750,000 psi. Other conditions remained standard. The fatigue lives of ball groups having hardnesses of 59, 60, and 62 on the Rockwell C scale are given in figures 5(a) to (c). For comparative purposes a second line showing actual life was adjusted to that expected at the standard test stress. This adjustment was made according to the inverse 10^{th} power relation between life and stress previously reported for the spin rig in reference 8. Figure 5(d) is a summary of these adjusted Weibull plots showing 10-percent failure lives at standard test conditions of 41×10^6 , 110×10^6 , and 350×10^6 stress cycles, respectively.

WB-49 balls. - This material was tested in the five-ball tester, where speed limitations were not a controlling factor over the wide range of hardness values investigated. Although the standard test conditions were employed, the rolling velocity and area of the running track were lower than in the spin rig and the amount of relative sliding between the contacting surfaces ($\omega_1 \sin \theta$, fig. 1(d)) was greater because of the effect of contact angle (fig. 1(d)).

Rolling-contact fatigue lives for groups of balls having Rockwell C hardnesses of 55, 60, 65, and 68 are given in figures 6(a) to (d). Figure 6(e) is a summary of Weibull plots for these specimen groups showing 10-percent failure lives of 1.7×10^6 , 4.3×10^6 , 5.8×10^6 , and 27.5×10^6 stress cycles, respectively.

Discussion of fatigue lives. - Figures 3(d), 4(e), and 5(d) show a continuous increase in 10-percent rolling-contact fatigue failure life, as measured in the fatigue spin rig, with increasing material hardness for AISI M-1, AISI M-50, and Halmo alloy steels, respectively. This trend was also present in the longer lived specimens, as measured by the 50-percent failure life for AISI M-1 and Halmo. At the highest hardness level, AISI M-50 had lower scatter than the other alloys and showed a reduced 50-percent life. The WB-49 five-ball-tester specimens (fig. 6(e)) showed an increase in both the 10-percent and 50-percent fatigue failure lives with increasing hardness. Early failure life (10 percent) is the more important criterion for evaluating the material because of the high degree of bearing reliability required in aircraft and spacecraft systems. Therefore, further discussion is based on the 10-percent failure life.

Figure 7 is a plot of 10-percent life against hardness for the three alloys studied in the fatigue spin rig (0° contact angle) and for WB-49 alloy studied in the five-ball tester (40° contact angle). Figure 7 shows that there is a general trend toward longer fatigue life with increased material hardness.

The results for AISI M-50 (fig. 4) are in good agreement with those given in reference 2, which show progressive increase in fatigue life with higher material hardness. These results are in contrast with the conclusions of reference 9, which assert that there is a maximum life for AISI M-50 at intermediate hardness values. However, the conclusions of reference 9 are based on a complex empirical life equation that must show a maximum, regardless of the experimental results, because of its assumed quadratic form. Only limited data are available at the hardness level (Rockwell C-64) producing the purported maximum in life. In reference 9, at the calculated optimum value of surface finish and grain size, no data were taken in the range above the optimum hardness where a deterioration in life is reported to exist. Data are not available at the intermediate hardness level (C-62) under the same test conditions as the C-64 data. Therefore, it is not possible to check the existence of a maximum directly without the use of the complex empirical quadratic form.

An important criterion of bearing strength is load-carrying capacity. Load-carrying capacity of the four alloys may be calculated at the various hardness levels from the fatigue-life results summarized in figure 7. Load capacity, contact load, and life are related by the equation

$$C = P \sqrt[n]{L_N}$$

where

C load capacity, or the contact load in pounds that will produce failure of 10 percent of the test specimens in one million stress cycles

P actual contact load in pounds

L_N actual 10-percent life in millions of stress cycles

n an exponent relating load and life, usually taken as 3 for bearing steels

Load capacity for each hardness level of the four alloys studied and the reductions in load capacity of softer specimen groups relative to the hardest groups are given in the following table (the variations in contact load P are due to differences in geometrical conformity):

| Material | Hardness, Rockwell C- | P | L_N (fig. 7) | C | Ratio of C to hardest in group |
|--------------------------------|--------------------------|-----|-------------------|------|--------------------------------------|
| AISI M-1 (spin rig) | 62 | 875 | 97 | 4020 | 0.518 |
| | 64.5 | 875 | 570 | 7240 | .934 |
| | 66 | 875 | 695 | 7750 | 1.000 |
| AISI M-50 (spin rig) | 60 | 875 | 65 | 3520 | 0.711 |
| | 60.5 | 875 | 116 | 4270 | .862 |
| | 62 | 875 | 176 | 4890 | .989 |
| | 63 | 875 | 182 | 4950 | 1.000 |
| Halmo (spin rig) | 59 | 875 | 41 | 3070 | 0.498 |
| | 60 | 875 | 110 | 4160 | .676 |
| | 62 | 875 | 350 | 6160 | 1.000 |
| WB-49 (five-ball tester) | 55 | 173 | 1.7 | 206 | 0.394 |
| | 60 | 173 | 4.3 | 281 | .538 |
| | 65 | 173 | 5.8 | 303 | .580 |
| | 68 | 173 | 27.5 | 522 | 1.000 |

These calculations show that a large variation in load capacity may be produced by control of material hardness within the range (above C-58) applicable to bearing steels and that the highest hardness of a given alloy shows the highest load capacity. Although life data in this table are for the same contact stress, specimen loads producing this stress varied because of differences in contact geometry; and thus load capacities for tests run under different ball loads cannot be compared directly. The improvement in load capacity with higher hardness shown in this table has been observed experimentally with full-scale bearings. Figure 8 shows the load capacity as a function of hardness for SAE 52100 steel bearings tested by the Marlin-Rockwell Corporation along with the results of the present investigation, which are included for comparative purposes.

Effect of Hardness on Mechanical Strength

Several investigators have reported an increase in mechanical-strength properties such as elastic limit, yield strength, and ultimate strength in both tension and compression with increasing material hardness (refs. 3 and 10). At hardness values approaching the ultimate attainable hardness for a given alloy composition, these investigators have observed a peak in the measured strength values and subsequent loss in measured strength at higher hardness values. These observations suggest a possible maximum in rolling-contact fatigue life at an intermediate hardness level close to the maximum for a particular alloy.

As a part of a coordinated research effort, of which the fatigue data reported herein are a portion, the elastic limit, yield strength, and ultimate strength in both tension and compression as a function of hardness were measured for bar specimens from the same material heats of AISI M-1, AISI M-50, and Halmo as were used to produce the rolling-contact fatigue data reported in figures 3, 4, and 5. Figures 9 and 10 are plots of mechanical strength in tension and compression, respectively, for these alloys. These data were previously published in references 5 and 6. Trends similar to those shown in references 3 and 10 were observed. In general, an increase in mechanical strength with higher hardness was observed up to an optimum hardness, after which strength tended to deteriorate at very high hardness values. This deterioration in strength could be produced by minor eccentricities in loading that would cause higher than nominal stresses in very hard specimens and hence produce an apparent loss in strength. As stated by the authors of reference 5, the deterioration in strength at very high hardness may be due to residual stresses not relieved at the low tempering temperature used to produce the highest material hardnesses. An indication that residual stresses are not responsible for loss in strength at very high hardness is provided by the SAE 52100 data given in references 5 and 6. This steel shows maximum strength at an intermediate hardness, as do the tool steels in figures 9 and 10. However, rotating-beam fatigue-life results for this 52100 steel given in references 5 and 6 do not show a maximum at an intermediate hardness. Since residual stresses are in tension at the surface and therefore additive in the rotating-beam test, a maximum at an intermediate hardness and subsequent loss in life at the highest hardnesses would be anticipated if residual stresses of significant magnitude were present. The fact that no loss in rotating-beam fatigue life was observed at very high hardnesses indicates that residual stresses are not the primary cause of loss in strength of very hard bar specimens.

The apparent decrease of elastic modulus at higher hardness values (fig. 11) may be further evidence of overstressing due to eccentric loading. These results (from ref. 6) are for the same heats of material as the bar specimens of figures 9 and 10 and the ball specimens of figures 3 to 5. Higher than nominal stresses would produce a greater amount of strain and hence reduce the ratio of nominal stress to actual strain, which is the measured elastic modulus.

The observed mechanical strength properties from references 5 and 6 do not correlate with the observed rolling-contact fatigue life resulting for AISI M-1, AISI M-50, and Halmo. Mechanical strength was highest at an optimum intermediate hardness and somewhat lower at the highest hardness values, while fatigue life improved continuously with higher hardness. This may be due to a true lack of correlation between mechanical strength and fatigue life, or to the presence of undetected stress concentrations caused by eccentricities in loading of the hardest tension and compression test specimens.

Deformation and Wear Studies

Spin-rig specimens. - Wear and plastic-deformation volumes for three 1/2-inch AISI M-1 spin-rig ball specimens having hardnesses of Rockwell C 62, 64.5, and 66 were measured from transverse surface profile traces (fig. 2) of the ball's running track. These specimens were run for 1.7×10^9 stress cycles under the same test conditions as the AISI M-1 fatigue specimens reported in figure 3. Figure 12 is a plot of wear and deformation volume as a function of ball hardness. A general trend toward decreased wear and deformation volume with higher material hardness is observed.

Five-ball tester specimens. - Balls of 1/2-inch diameter from each of the three hardness levels of AISI M-1, AISI M-50, and Halmo tool steels and the two highest hardness levels of WB-49 steel were run in the five-ball fatigue tester as wear and deformation specimens. These balls were run at a 40° contact angle to a total of 10,000 stress cycles under a load that produced 750,000-psi maximum theoretical (Hertz) compressive stress. Wear and deformation volumes were measured from transverse surface profile traces of the ball's running track. Figures 13(a) to (d) are plots of these volumes against material hardness. In each case a general trend toward decreased wear and deformation volume with higher material hardness was observed.

Discussion of deformation and wear results. - The plastic deformation measurements compiled in figures 12 and 13 offer a possible method of checking the validity of the mechanical-strength results at high material hardness. Elastic limit and yield strength are measures of the susceptibility of a material to plastic deformation. Thus, a decrease in actual elastic limit and mechanical strength should be accompanied by an increase in the degree of plastic deformation. Figures 12 and 13 show that the hardest specimen from each of the four alloys showed the least volume of plastic deformation. This indicates an increase in the actual elastic limit and yield strength at hardness levels in the range where tension and compression tests showed a decrease in these properties. The deformation measurements were made from spherical specimens that are of necessity concentrically loaded. The conflicting results with sphere and bar specimens may be due to extraneous bending stresses generated by eccentric loading in the bar specimens. Actual elastic limit and yield strength may continue to increase at the highest hardness levels, contrary to the apparent trends established with bar specimens in tension and compression.

The continuous improvement in resistance to plastic deformation of AISI M-1, AISI M-50, and Halmo with higher material hardness does correlate with the observed upward trends of rolling-contact fatigue life for those materials. Thus, while the true elastic limit may correlate with fatigue life, inherent difficulties in testing very hard bar specimens may preclude an accurate determination of the true elastic limit.

E-524

CB-2 back

The increased resistance to mechanical wear shown in figures 12 and 13 agrees with previously reported theoretical and experimental results. Burwell in reference 11 states that wear volume for a given material, load, and distance of sliding is proportional to the reciprocal of hardness. The experimental results reported in reference 12 show a decrease in wear volume with higher material hardness.

Metallographic Structure

The different tempering temperatures used to produce the variation in hardness for each of the four materials studied produced only minor modifications in metallographic structure. Photomicrographs of these structures are shown in figures 14 to 17. The softer balls tended to have larger, more numerous precipitated carbides and greater definition of tempered martensite. Previous metallographic studies (ref. 13) have shown that carbides acting as stress raisers can cause severe localized matrix damage, which produces incipient fatigue cracking. Variation in carbide size and distribution caused by variations in tempering temperature may be an important contributor to the observed variations in fatigue life.

The percent by volume of retained austenite for these various heat treatments of the four alloys studied is given in table II. The percent retained austenite increased with decreasing tempering temperature and increasing material hardness.

One of the practical requirements of a bearing-material heat-treatment schedule is control of retained austenite. Volume changes resulting from in-service austenite transformation are detrimental to precision bearing operation. Castleman, Averbach, and Cohen (ref. 14) have shown that retained austenite has a deleterious effect on mechanical-strength properties in AISI 2340 steel. Thus, aside from the volume-change problem, the percentage of retained austenite in the microstructure may influence rolling-contact fatigue life of tool steels. Since the amount of retained austenite is controlled by tempering temperature and is hence related to hardness, it is difficult to evaluate independently the effect of retained austenite on fatigue life. However, in the experiments reported herein, if there was any detrimental effect on fatigue life because of the presence of greater amounts of the soft retained austenite phase in the microstructure of the harder specimen groups, it was of lesser magnitude than the beneficial effect of the higher material hardness.

Cleanliness ratings for the four steels studied are given in table III. Prior austenite ASTM grain size is given in table II. Since only the tempering temperature was varied between specimen groups of each alloy, cleanliness and prior austenite grain size were held constant for each alloy composition.

Effect of Ball Hardness on Race Fatigue Life

The AISI M-1, AISI M-50, and Halmo ball specimens were run against race cylinders made, respectively, from the same heats of material. All race cylinders from a given alloy were given the same heat treatment; therefore, they had the same hardness and may be considered nominally identical. Figures 18 to 20 are Weibull plots of fatigue life for the three cylinder materials. Each was run against the groups of differing-hardness-level balls of the same alloy. Figures 18(d), 19(d), and 20(d) each show a slight increase in 10-percent fatigue failure life for cylinder specimens run against the harder ball groups.

CONCLUDING REMARKS

The rolling-contact fatigue studies reported herein show that life improves with increased material hardness. No optimum intermediate hardness or loss in life at very high hardness was observed. This relation between fatigue life and hardness has also been observed with full-scale bearings. Deformation studies also showed a continuous upward trend of resistance to plastic deformation with increased hardness paralleling the observed improvement in fatigue life. However, a continuous upward trend in mechanical strength was not observed with tension and compression tests of bar specimens made from the same material heats as the rolling-contact fatigue specimens.

It is of interest to note that the type of stress pattern produced in the bar specimens is fundamentally different from that which exists in contacting spherical bodies. Bar specimens have an equal stress distribution across the test specimen, and the stress is limited by the strength of the material. Contacting spherical bodies deflect from the initial point contact to produce a finite contact area that supports the applied load. The pressure profile is elliptical across the contact area, varying from zero at the edge to a maximum at the center. This maximum pressure may be much higher than the yield strength of the material. Gross plastic deformation is avoided because of confinement of the localized, highly stressed material by the surrounding unstressed material outside the contact area. However, relatively small amounts of permanent plastic deformation are detectable in rolling-contact specimens after repeated rolling on the same track. This is a potential fatigue mechanism, since it involves successive disruptions of the metallic crystal structure. Plastic deformation can take place, although on a much smaller scale, at stress levels within the normal bearing operating range (ref. 15).

The stress pattern of an indentation hardness test and the plastic deformation it produces are somewhat similar to those of rolling spheres, only more severe. Hardness is a measure of mechanical strength under conditions approximating that of bodies in rolling contact. Thus, hardness or a simple plastic deformation test with a rolling-contact element may be a more valid estimate of relative fatigue life for different heat treatments of a given alloy than tension or compression tests of bar specimens.

SUMMARY OF RESULTS

The fatigue spin rig and the five-ball tester were used to determine the rolling-contact fatigue life of groups of AISI M-1, AISI M-50, Halmo, and WB-49 alloy steel balls tempered to various hardness levels. Tests were run at room temperature and 800,000-psi maximum theoretical (Hertz) compressive stress with a synthetic diester lubricant, Mil-L-7808. Material hardness, resistance to plastic deformation of specimen in rolling contact, and previously published tensile and compressive strength data for bar specimens for these same heats of material were compared with the fatigue-life results. The following results were obtained:

1. Rolling-contact fatigue life and load-carrying capacity of each of the four alloy compositions studied increased continuously with higher material hardness. The improvement in load capacity was in the order of 30 to 100 percent over the hardness range tested. No maximum fatigue life or load capacity at intermediate hardness values was observed.

2. These fatigue results did not correlate with previously published tension and compression strength results for bar specimens from the same heats of material, which showed an apparent optimum strength at intermediate hardness values. This may be due to a true lack of correlation between fatigue life and mechanical strength or to errors in loading of the hardest tension and compression specimens.

3. Resistance to permanent plastic deformation of specimens in rolling contact showed a general increase with increasing hardness. Since the stress pattern in a hardness test is similar to that of bodies in rolling contact, some measure of resistance to plastic deformation may be a qualitative estimate of relative fatigue lives of different heat treatments of a given alloy composition.

4. Only minor differences in metallographic structure were observed for the various hardness levels of each alloy considered. The softer balls tended to have more and larger fine (precipitated) carbides and greater definition of tempered martensite. Percent retained austenite increased with higher hardness (lower tempering temperature).

Lewis Research Center

National Aeronautics and Space Administration

Cleveland, Ohio, December 9, 1959

APPENDIX - STRESS-CYCLE RELATION

The following symbols, shown in figure 1(d), are used in this derivation:

- r radius of ball specimen and lower support balls
 v_1 surface tangential velocity of test specimen at point of contact
 v_2 tangential velocity of support balls
 ω_1 angular velocity of drive shaft
 ω_2 angular velocity of support balls around center of shaft axis
 θ contact angle

The relative speed of the test specimen and the lower support balls is derived as follows:

$$v_1 = \omega_1 r_1 \quad (r_1 = r \cos \theta)$$

$$v_1 = \omega_1 r \cos \theta$$

$$v_2 = \frac{v_1}{2} \quad (r_2 = 2r \cos \theta)$$

$$\omega_2 = \frac{v_2}{r_2} = \frac{v_2}{2r \cos \theta}$$

$$\omega_2 = \frac{v_1}{4r \cos \theta}$$

$$\omega_2 = \frac{\omega_1 r \cos \theta}{4r \cos \theta}$$

$$\omega_2 = \frac{\omega_1}{4}$$

The relative angular velocity of the upper ball to a lower ball is $\omega_1 - \omega_2 = 3\omega_1/4$. The upper ball receives 3/4 of a stress cycle per revolution from each lower ball. Therefore, the number of stress cycles per revolution equals 3/4 stress cycles per ball multiplied by 4 balls, or 3 stress cycles; that is, a point on the upper ball is stressed three times per shaft revolution.

REFERENCES

1. Hamaker, John C., Jr., Strang, Vance C., and Roberts, George A.: Bend: Tensile Relationships for Tool Steels at High Strength Levels. Trans. ASM, vol. 49, 1957, pp. 550-573; discussion, pp. 573-575.
2. Jackson, E. G.: Rolling Contact Fatigue Evaluation of Bearing Materials and Lubricants. Trans. ASLE vol. 2, no. 1, 1959, p. 121.
3. Muir, Hugh, Averbach, B. L., and Cohen, Morris: The Elastic Limit and Yield Behavior of Hardened Steels. Trans. ASM, vol. 47, 1955, pp. 380-399; discussion, pp. 399-407.
4. Macks, E. F.: The Fatigue Spin Rig - A New Apparatus for Rapidly Evaluating Materials and Lubricants for Rolling Contact Bearings. Lubrication Eng., vol. 9, no. 5, Oct. 1953, pp. 254-258.
5. Sachs, G., Sell, R., and Brown, W. F.: Tension, Compression and Fatigue Properties of Several Steels for Aircraft Bearing Applications. Paper No. 73, ASTM, 1959.
6. Sachs, G., Sell, R., and Weiss, V.: Tension, Compression, and Fatigue Properties of Several SAE 52100 and Tool Steels Used for Ball Bearings. NASA TN D-239, 1960.
7. Jones, A. B.: New Departure - Analysis of Stresses and Deflections. Vols. I and II. New Departure, Div. General Motors Corp., Bristol (Conn.), 1946.
8. Butler, Robert H., and Carter, Thomas L.: Stress-Life Relation of the Rolling-Contact Fatigue Spin Rig. NACA TN 3930, 1957.
9. Baughman, R. A.: Effect of Hardness, Surface Finish, and Grain Size on Rolling Contact Fatigue Life of M-50 Bearing Steel. Paper No. 59-LUB-11, ASME, 1959.
10. Grobe, Arthur H., and Roberts, George A.: The Bend Test for Hardened High Speed Steel. Trans. ASM, vol. 40, 1948, pp. 435-471.
11. Burwell, John T., Jr.: Survey of Possible Wear Mechanisms. Wear, vol. I, no. 2, Oct. 1957, pp. 119-141.
12. Pomey, J.: Friction and Wear. NACA TM 1318, 1952.
13. Bear, H. Robert, and Butler, Robert H.: Preliminary Metallographic Studies of Ball Fatigue Under Rolling-Contact Conditions. NACA TN 3925, 1957.

14. Castleman, L. S., Averbach, B. L., and Cohen, Morris: Effect of Retained Austenite Upon Mechanical Properties. Trans. ASM, vol. 44, 1952, pp. 240-257; discussion, pp. 257-263.
15. Moyar, G. J., and Morrow, JoDean: Relation of Fatigue to Pitting Failure of Surfaces in Rolling Contact. Dept. Theoretical and Appl. Mech., Univ. Ill., Dec. 1958.

E-524

CB-3

TABLE I. - ANALYSIS OF TEST MATERIALS

| Material | Analysis, percent by weight | | | | | | | | | | |
|-----------|-----------------------------|-------|-------|------|------|------|------|------|------|------|-----|
| | C | P | S | Mn | Si | Cr | V | W | Mo | Ni | Co |
| AISI M-1 | 0.80 | 0.004 | 0.007 | 0.25 | 0.32 | 3.76 | 1.15 | 1.53 | 8.54 | 0.07 | --- |
| AISI M-50 | .81 | .004 | .007 | .26 | .14 | 3.97 | 1.07 | .01 | 4.29 | .05 | --- |
| Halmo | .59 | .005 | .007 | .31 | 1.10 | 4.79 | .51 | ---- | 5.22 | ---- | --- |
| WB-49 | 1.07 | .006 | .007 | .30 | .02 | 4.4 | 2.0 | 6.8 | 3.9 | .04 | 5.2 |

E-524

CB-3 back

TABLE II. - TEST MATERIAL PROPERTIES AND HEAT TREATMENT

[Melting process, induction vacuum.]

| Material | Hardness, Rockwell C - | Retained austenite, percent by volume | Austenitic grain size, ASTM | Heat treatment | | | | | 3rd Temper (40 min), OF |
|-----------|------------------------------|--|--------------------------------------|--|---------------------------|---------------------------|--------------------------------|--------------------------------|-------------------------------|
| | | | | Preheat, OF | Austenitize, OF | Quench, OF | 1st Temper (120 min), OF | 2nd Temper (120 min), OF | |
| AISI M-1 | 62 | 2.8 | 8- | Salt: 1450, $3\frac{1}{2}$ min ↓ | 2200 ↓ | Oil: 120 ↓ | 1100 | 1100 | ---- |
| | 64.5 | 3.2 | | | | | 1050 | 1050 | ---- |
| | 66 | 7.2 | | | | | 1000 | 1000 | ---- |
| AISI M-50 | 60 | 1.8 | 8- | Salt: 1450, $3\frac{1}{2}$ min ↓ | 2050 ↓ | Oil: 120 ↓ | 1100* | 1100 | ---- |
| | 60.5 | 2.2 | | | | | 1050 | 1050 | ---- |
| | 62.0 | --- | | | | | 1000 | 1000 | 1025 |
| | 63 | 4.2 | | | | | 1000 | 1000 | ---- |
| Halmo | 59 | 2.6 | 6 to 7 | Salt: 1450, $3\frac{1}{2}$ min ↓ | 2100 ↓ | Oil: 120 ↓ | 1100 | 1100 | ---- |
| | 60 | 3.6 | | | | | 1050 | 1050 | ---- |
| | 62 | 4.4 | | | | | 1000 | 1000 | ---- |
| WB-49 | 55 | < 1 | 8+ | Salt: 1500, 6 min ↓ | Salt: 2225, 6 min ↓ | Salt: 1225, 6 min ↓ | 1025 | 1025 | 1250 |
| | 60 | < 1 | | | | | | ↓ | 1200 |
| | 65 | < 1 | | | | | | | 1150 |
| | 68 | 5.0 | | | | | | | ---- |

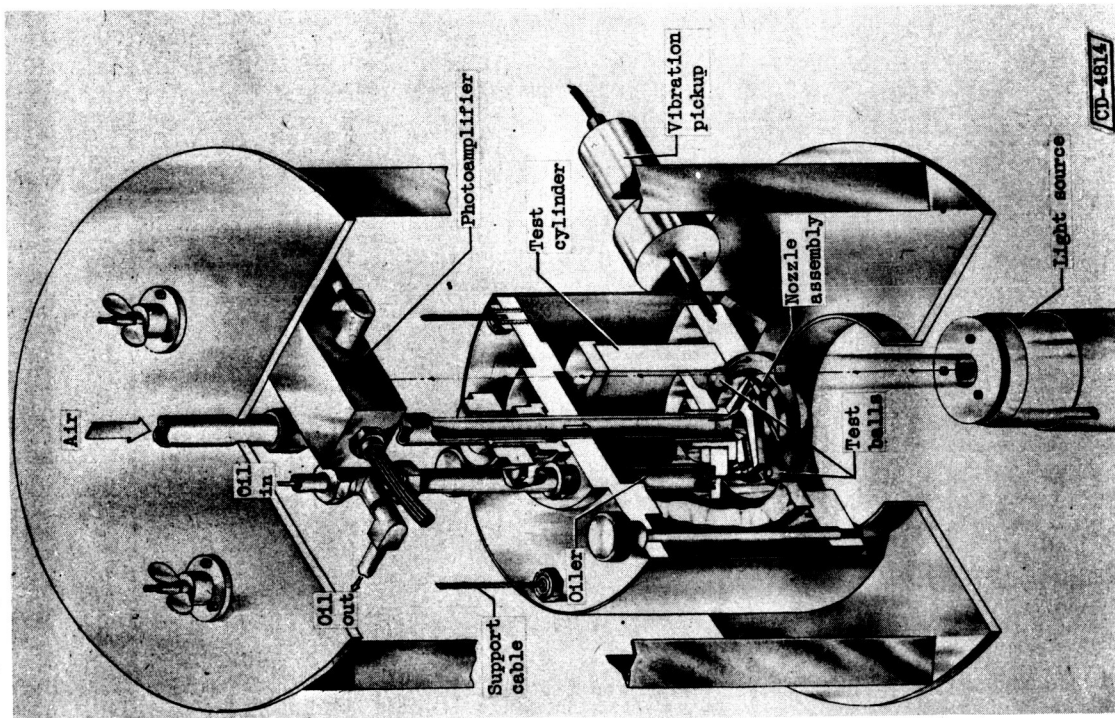
TABLE III. - NONMETALLIC INCLUSION RATINGS
OF TEST MATERIALS

[Jernkontoret charts (ASTM spec. E45-51).]

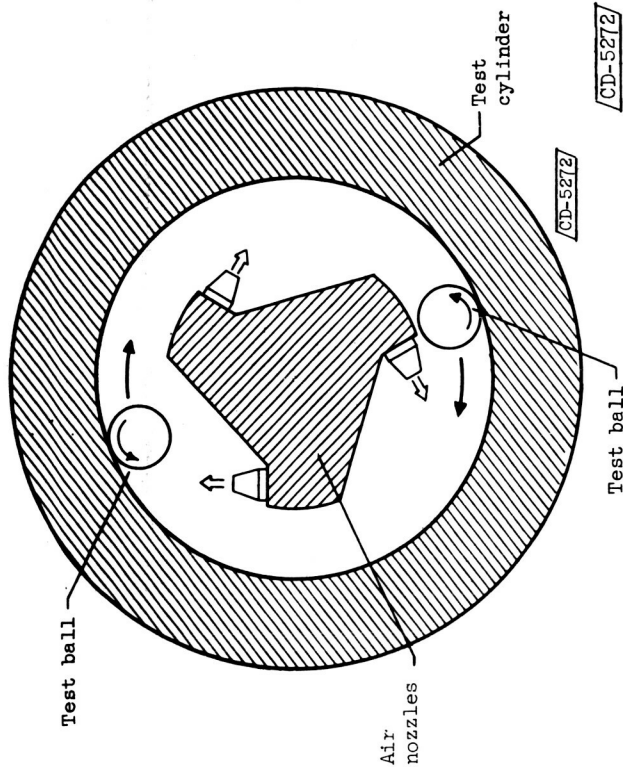
| Material | Thin series ^a | | | | Thick series ^a | | | |
|-----------|--------------------------|-----|----|-----|---------------------------|-----|---|-----|
| | A | B | C | D | A | B | C | D |
| AISI M-1 | 0 | 1.0 | 0 | 1.5 | 0 | 0 | 0 | 0 |
| AISI M-50 | .5 | 1.5 | .5 | 2.0 | 0 | .5 | 0 | .5 |
| Halmo | .5 | 2.0 | .5 | 2.0 | 0 | 0 | 0 | .5 |
| WB-49 | 1.5 | 0 | 0 | 1.0 | - | --- | - | --- |

^aDesignation:

- A sulfides
- B aluminates
- C silicates
- D oxides

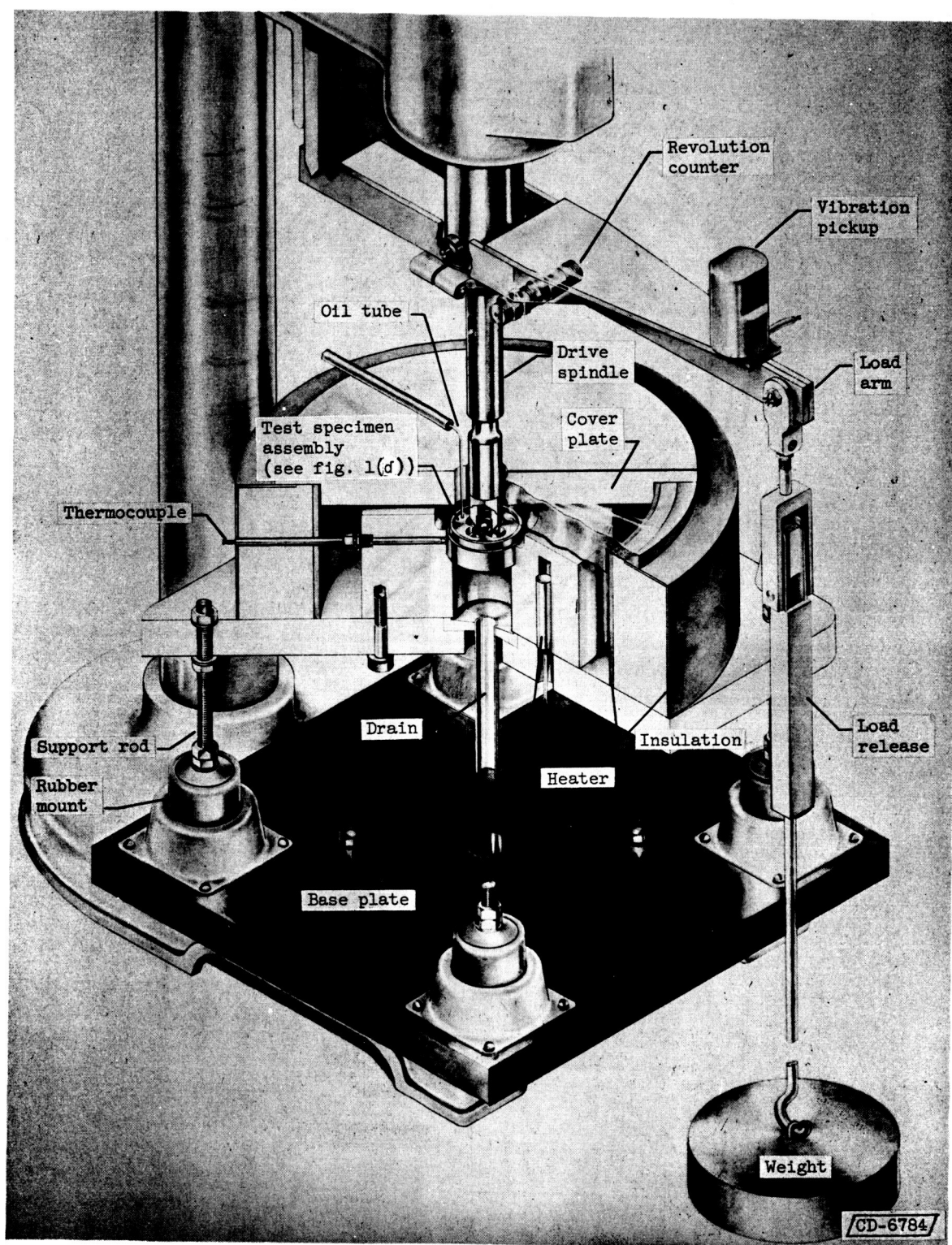


(a) Cutaway view, rolling-contact fatigue spin rig.



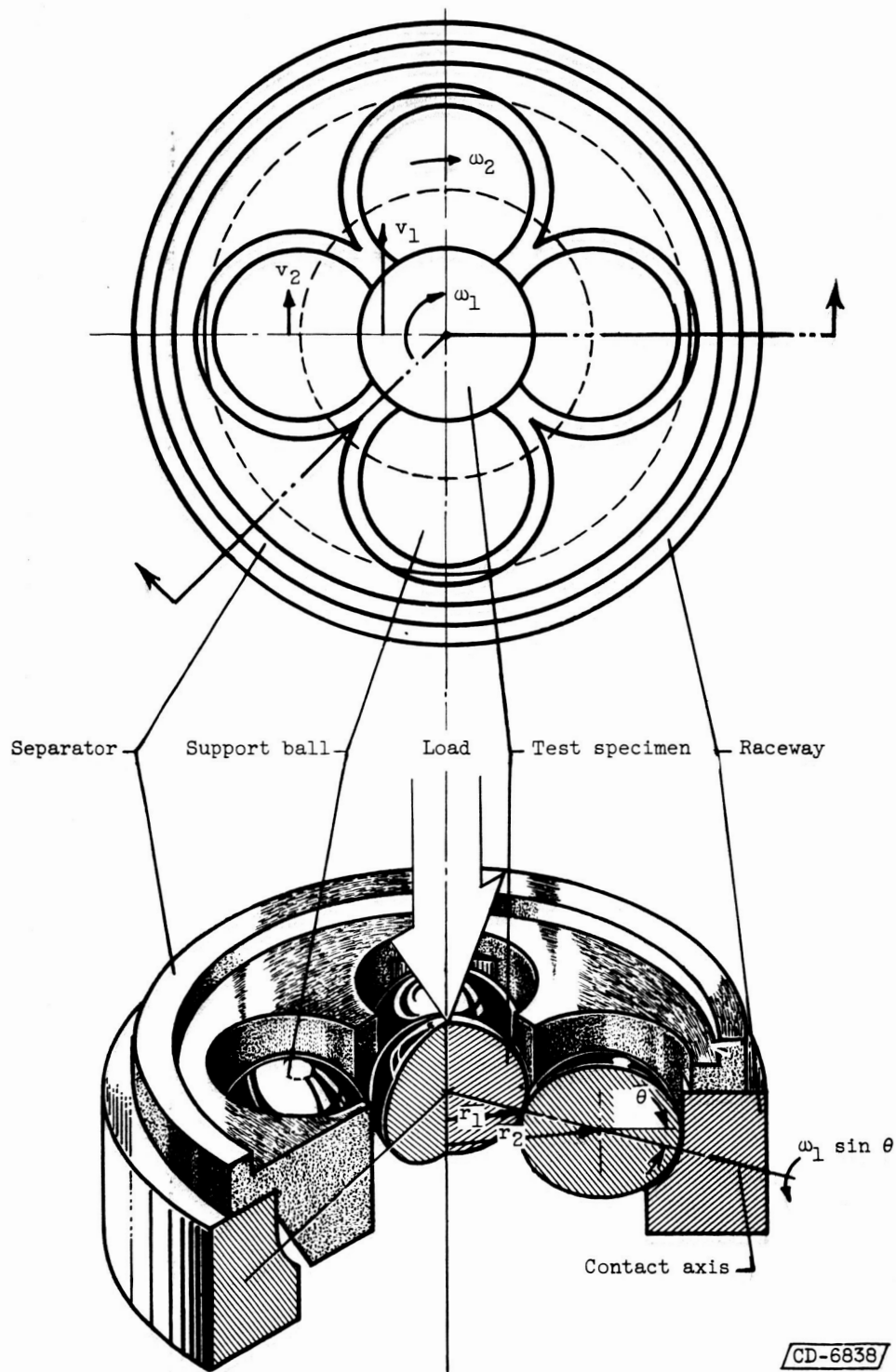
(b) Schematic diagram, rolling-contact fatigue spin rig.

Figure 1. - Test apparatus.



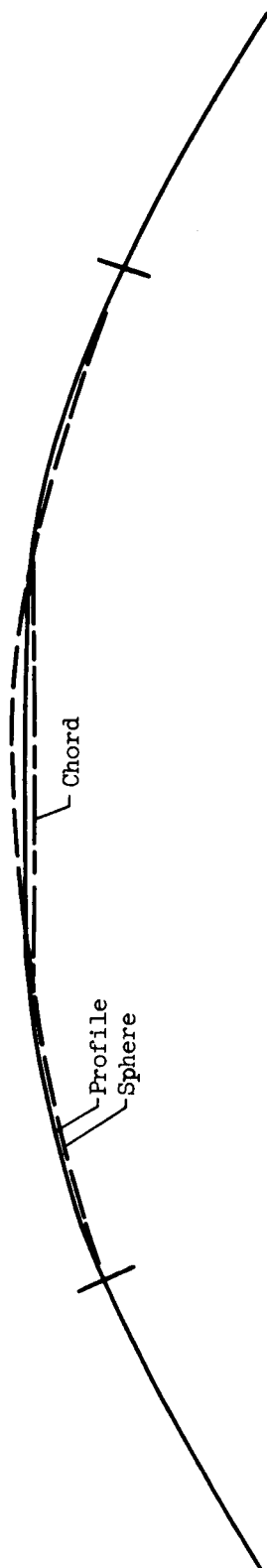
(c) Five-ball fatigue tester.

Figure 1. - Continued. Test apparatus.

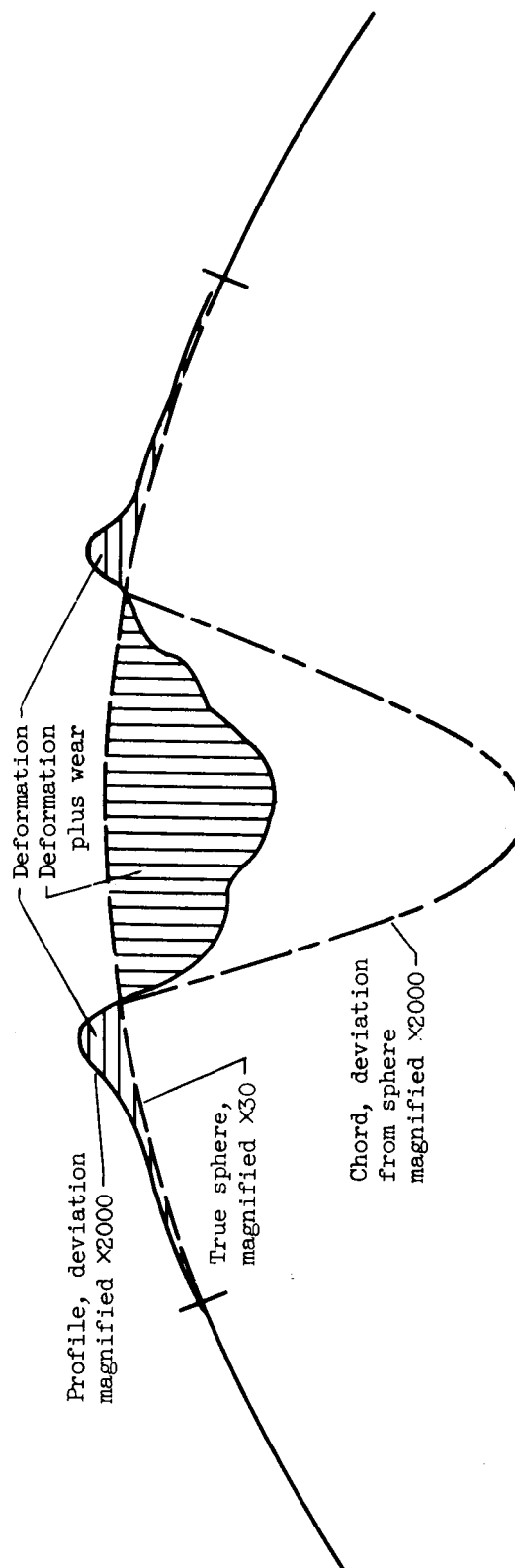


(d) Schematic diagram, five-ball fatigue tester.

Figure 1. - Concluded. Test apparatus.

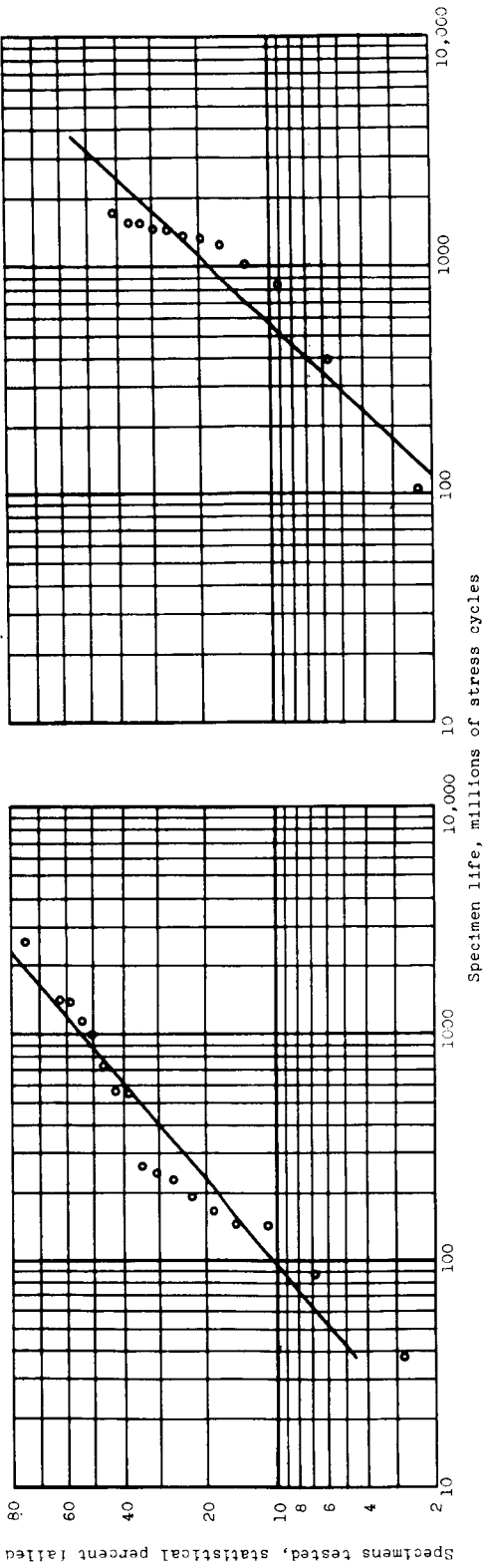


(a) Schematic cross section, sphere and deviation at same magnification.



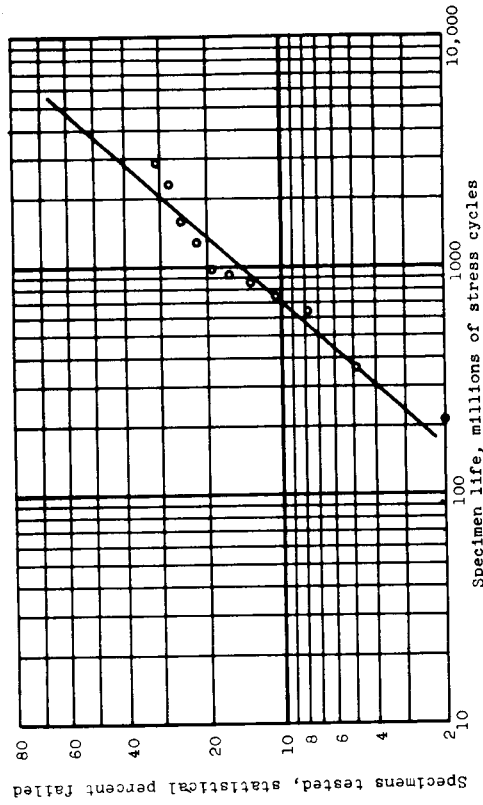
(b) Talyrond profile trace, deviation highly magnified.

Figure 2. - Cross section of postrun ball specimen track (not to scale).



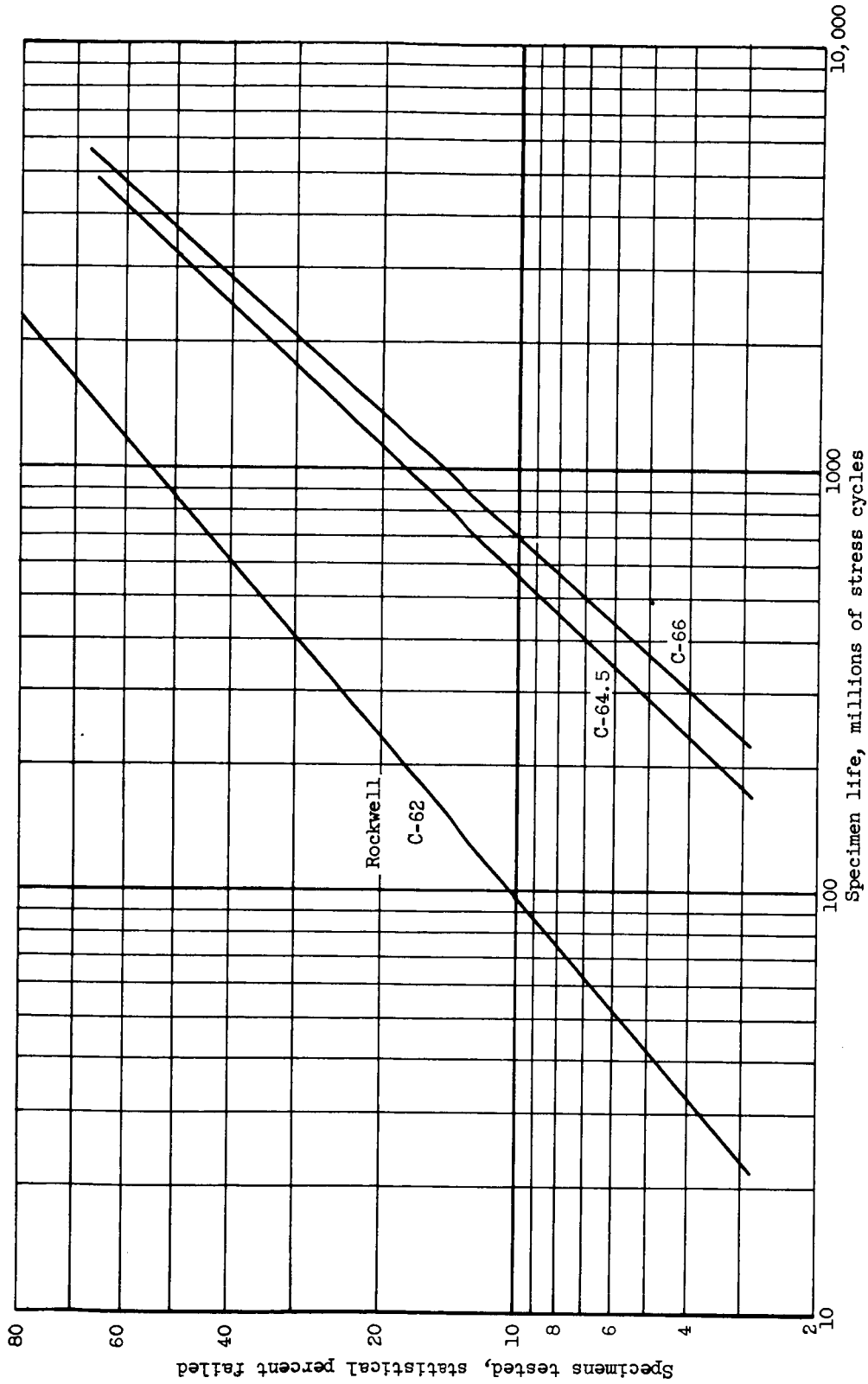
(a) Rockwell C-62, double temper 2+2 hours at 1100° F.
Balls tested, 26; failed, 17.

(b) Rockwell C-64.5, double temper 2+2 hours at 1050° F.
Balls tested, 30; failed, 12.



(c) Rockwell C-66, double temper 2+2 hours at 1000° F.
Balls tested, 35; failed, 11.

Figure 3. - Rolling-contact fatigue life of AISI M-1 tool-steel balls tempered to various hardness levels. Maximum Hertz compressive stress, 800,000 psi; room temperature; diester lubricant; spin rig.



(d) Summary of fatigue lives for three hardness levels.

Figure 3. - Concluded. Rolling-contact fatigue life of AISI M-1 tool-steel balls tempered to various hardness levels. Maximum Hertz compressive stress, 800,000 psi; room temperature; diester lubricant; spin rig.

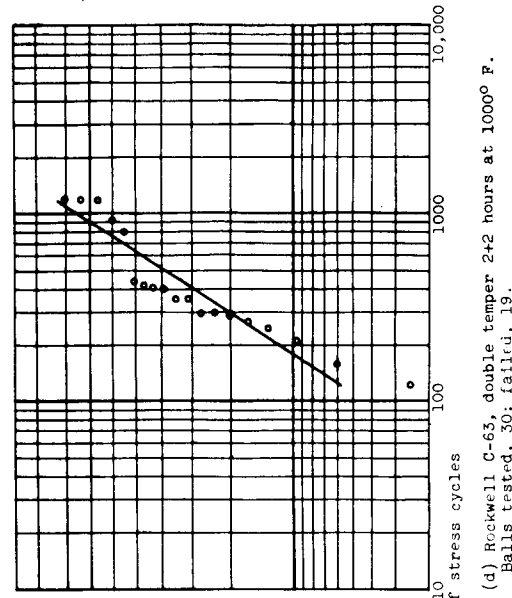
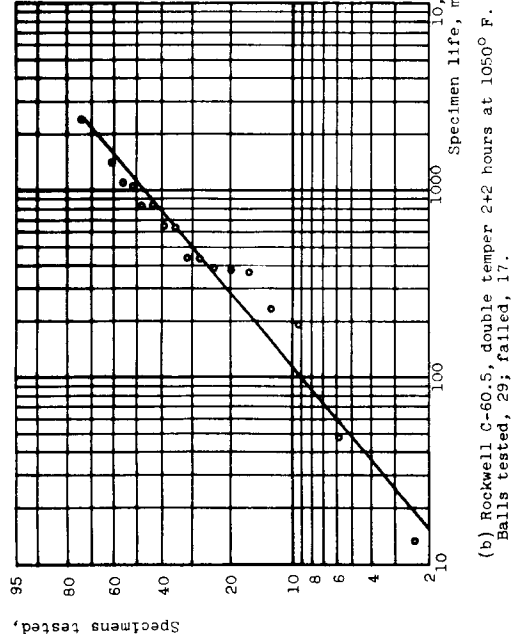
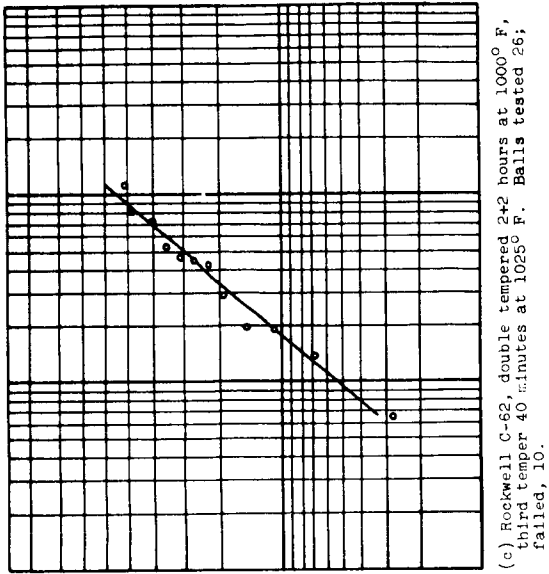
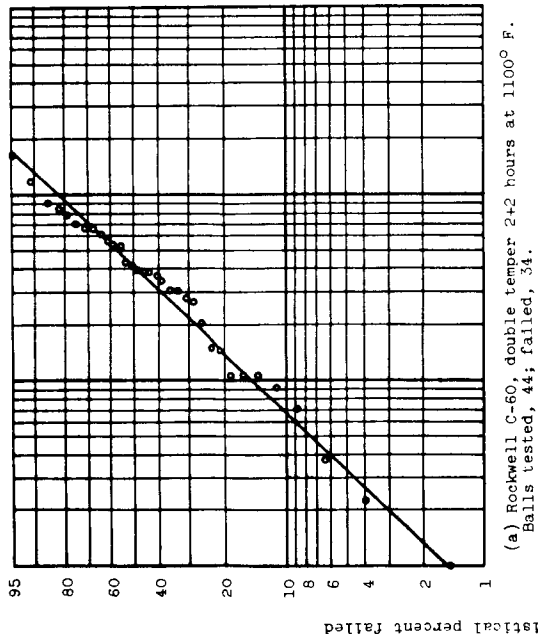
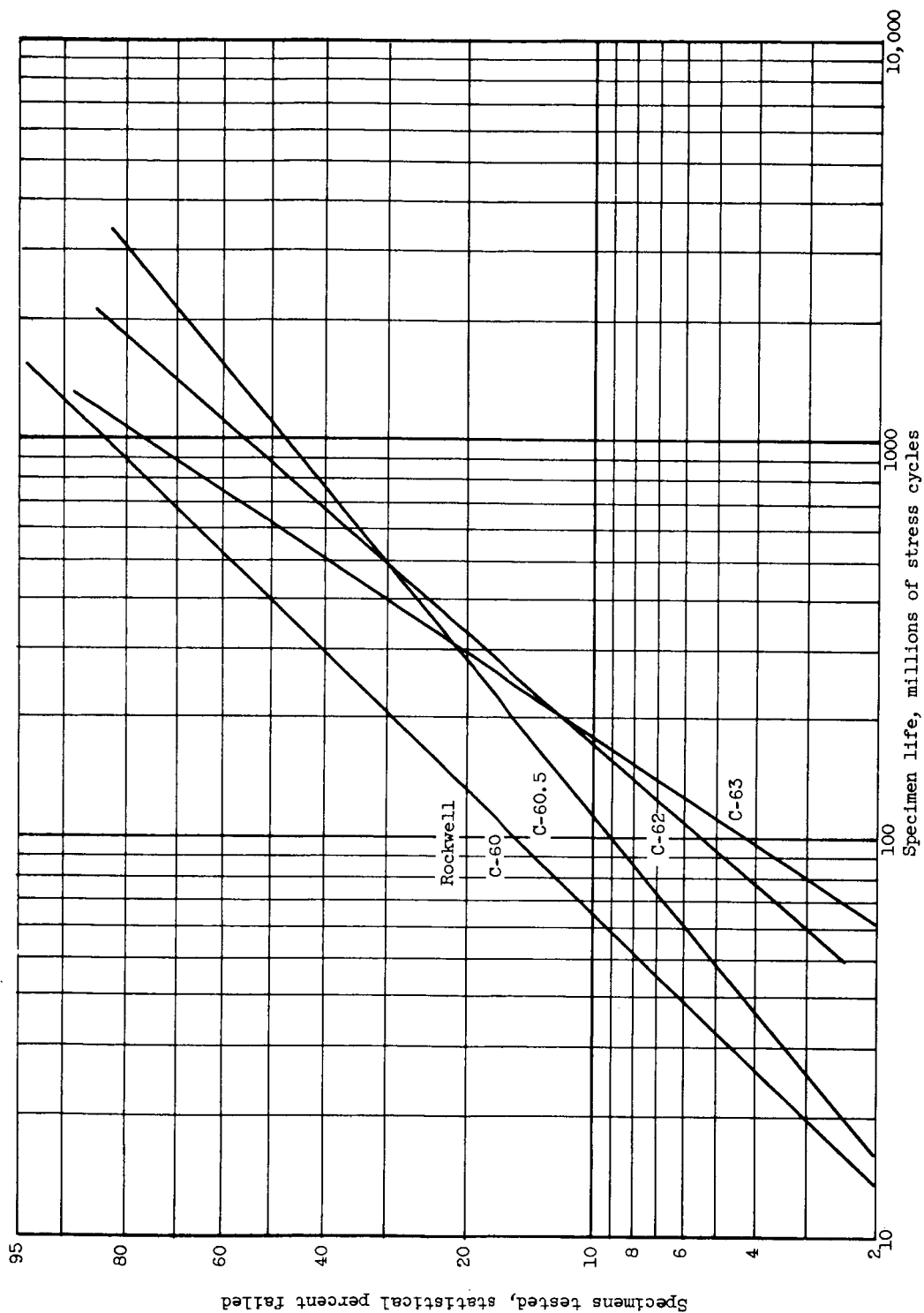
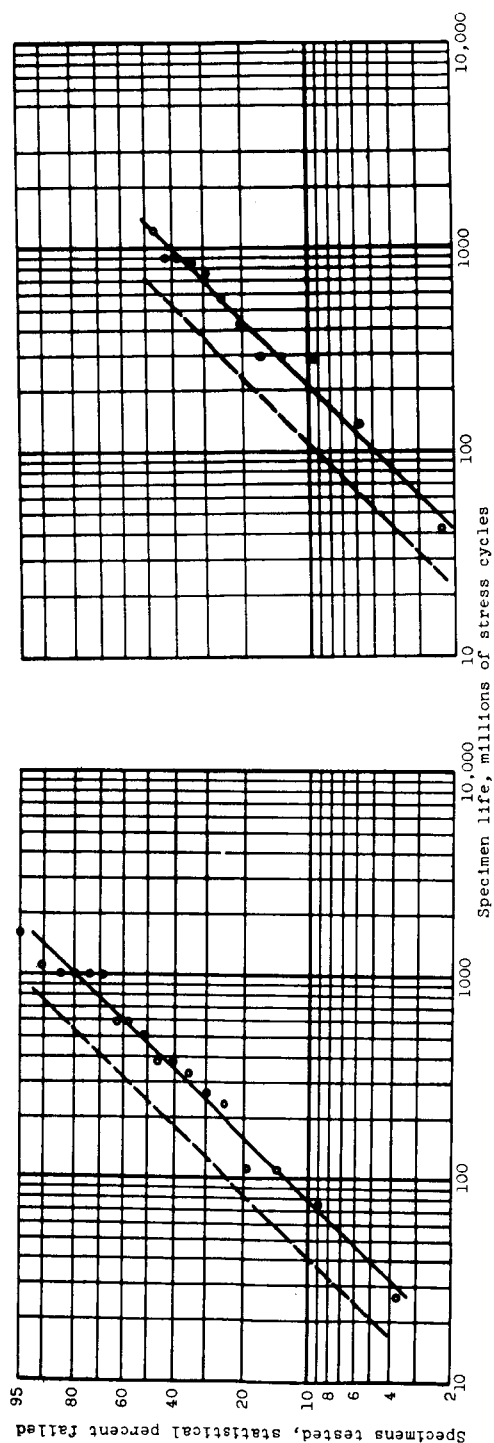


Figure 4. - Rolling-contact fatigue life of AISI M-50 tool-steel balls tempered to various hardness levels. Maximum Hertz compressive stress, 800,000 psi; room temperature; diester lubricant; spin rig.



(e) Summary of fatigue lives for four hardness levels.

Figure 4. - Concluded. Rolling-contact fatigue life of M-50 tool-steel balls tempered to various hardness levels. Maximum Hertz compressive stress, 800,000 psi; room temperature; diester lubricant; spin rig.



(b) Rockwell C-60, double temper 2+2 hours at 1050° F.
Balls tested, 30; failed, 12.

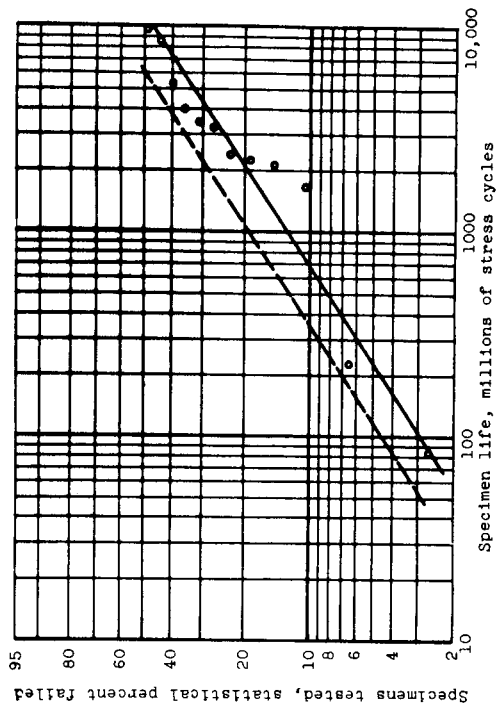
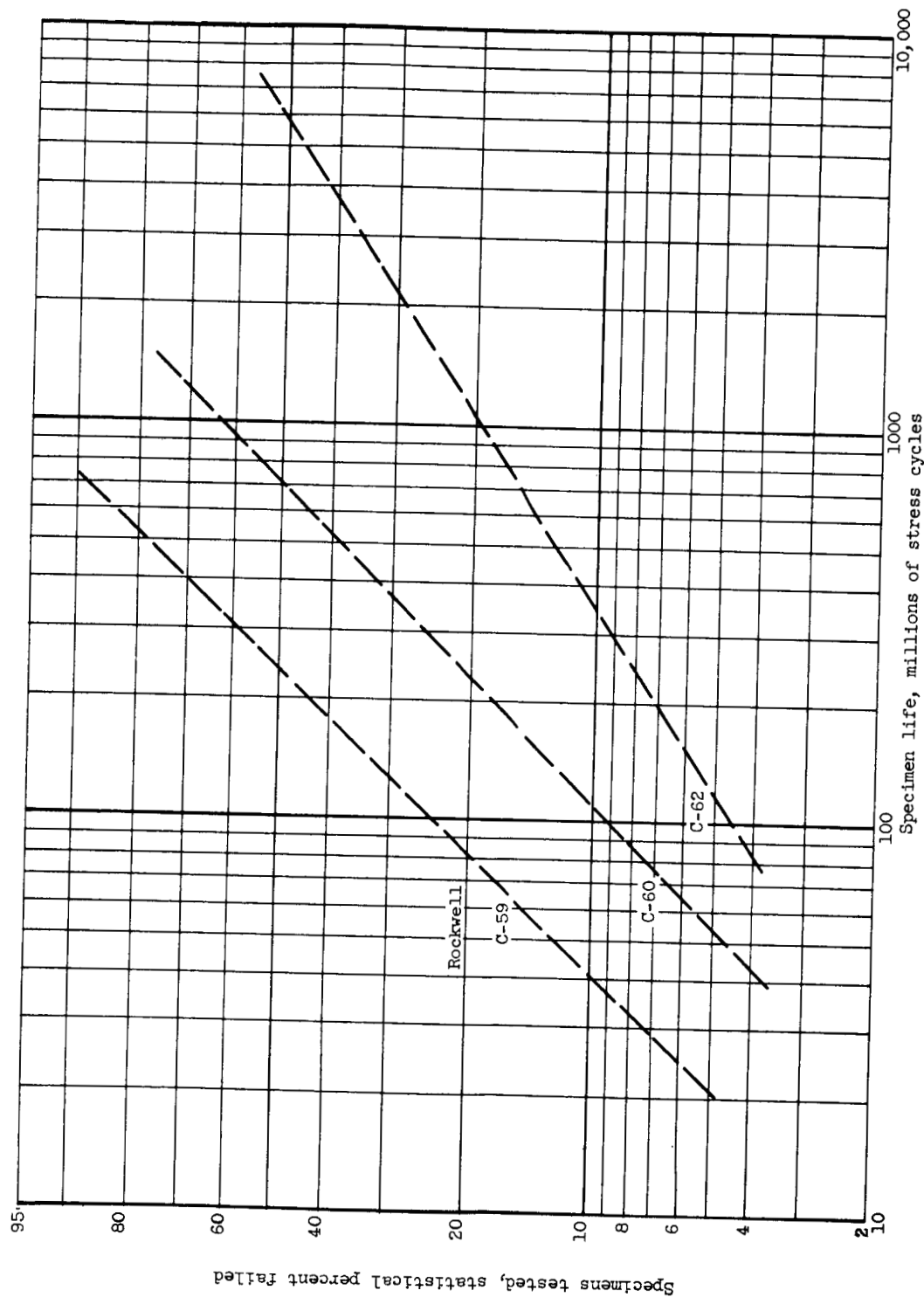
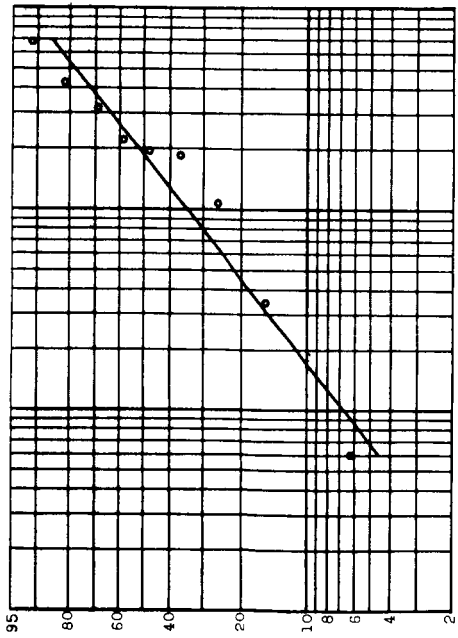


Figure 5. - Rolling-contact fatigue life of Halmo tool-steel balls tempered to various hardness levels. Maximum Hertz compressive stress, 750,000 psi; room temperature; diester lubricant; spin rig.

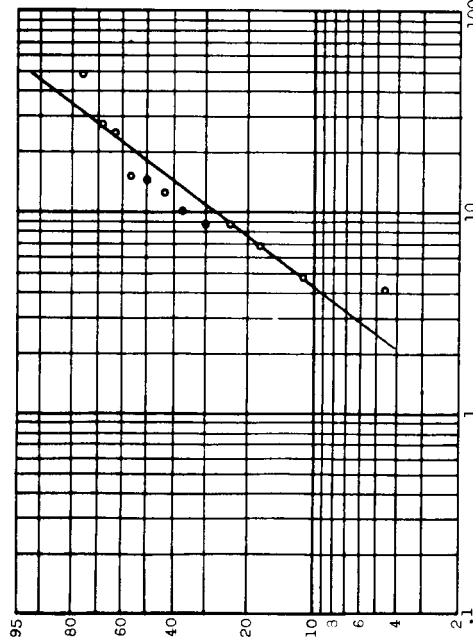


(d) Summary of fatigue lives for three hardness levels, adjusted to 800,000 psi stress.

Figure 5. - Concluded. Rolling-contact fatigue life of Halmo tool-steel balls tempered to various hardness levels. Maximum Hertz compressive stress, 750,000 psi; room temperature; diester lubricant; spin rig.

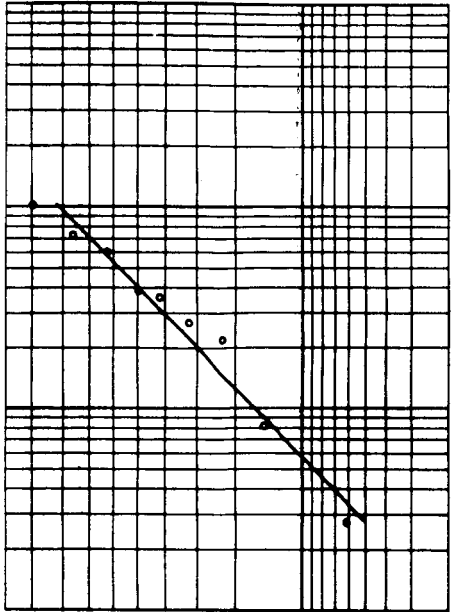


(a) Rockwell C-55, double temper 2+2 hours at 1025° F, third temper 40 minutes at 1250° F. Balls tested, 11; failed, 9.

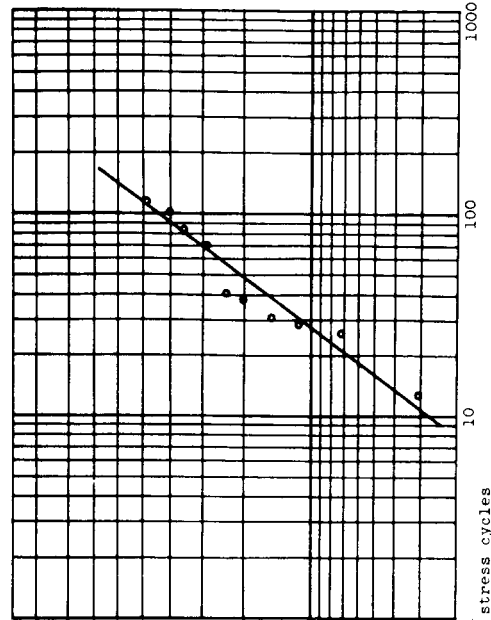


(b) Rockwell C-60, double temper 2+2 hours at 1025° F, third temper 40 minutes at 1200° F. Balls tested, 15; failed, 12.

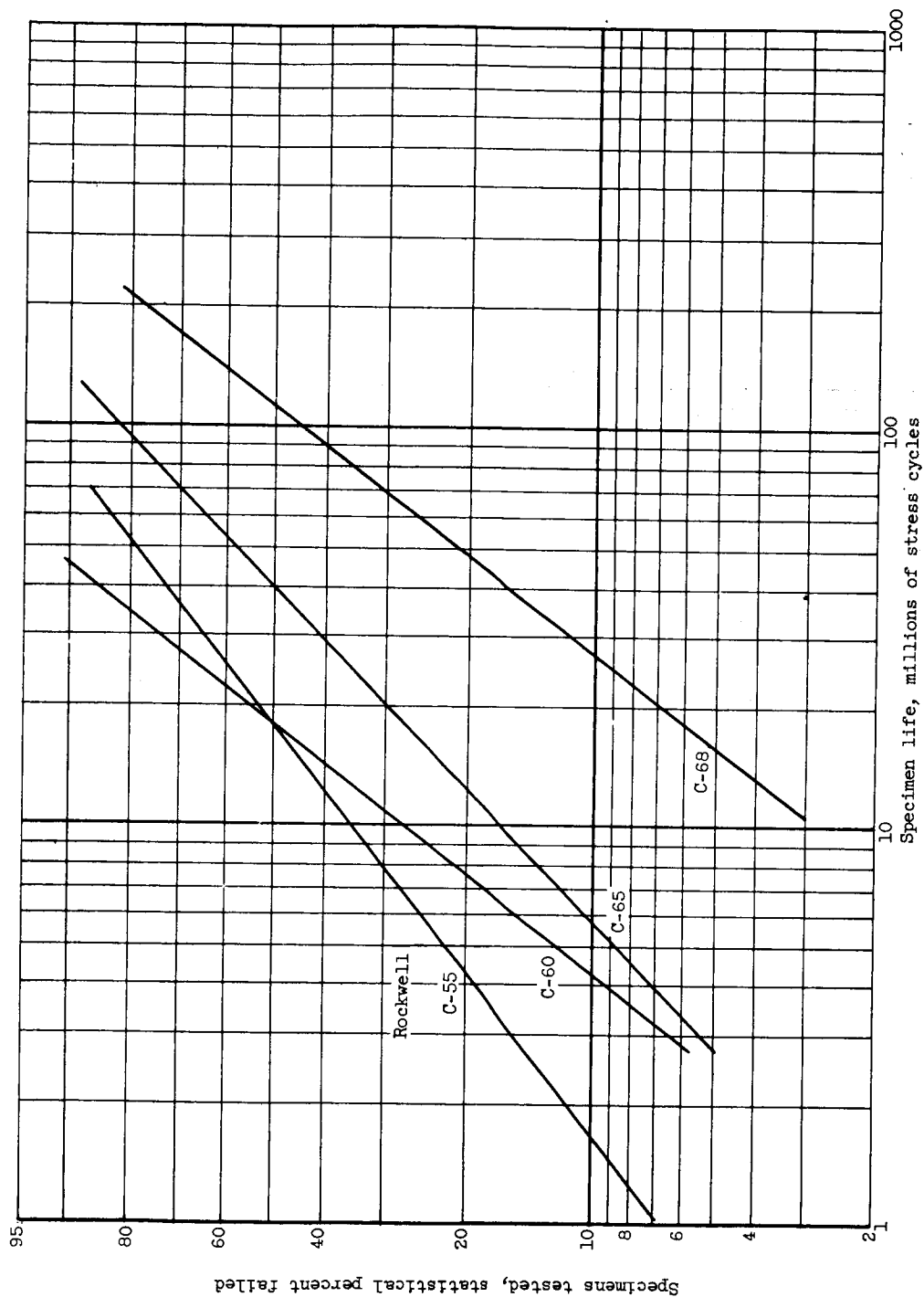
Figure 6. - Rolling-contact fatigue life of WB-49 tool-steel balls tempered to various hardness levels. Maximum Hertz stress, 800,000 psi; 40° contact angle; room temperature; diester lubricant; five-ball tester.



(c) Rockwell C-65, double temper 2+2 hours at 1025° F, third temper 40 minutes at 1150° F. Balls tested, 12; failed, 9.



(d) Rockwell C-68, double temper 2+2 hours at 1025° F. Balls tested, 20; failed, 10.



(e) Summary of fatigue lives for four hardness levels.

Figure 6. - Concluded. Rolling-contact fatigue life of WB-49 tool-steel balls tempered to various hardness levels. Maximum Hertz compressive stress, 800,000 psi; 40° contact angle; room temperature; diester lubricant; five-ball tester.

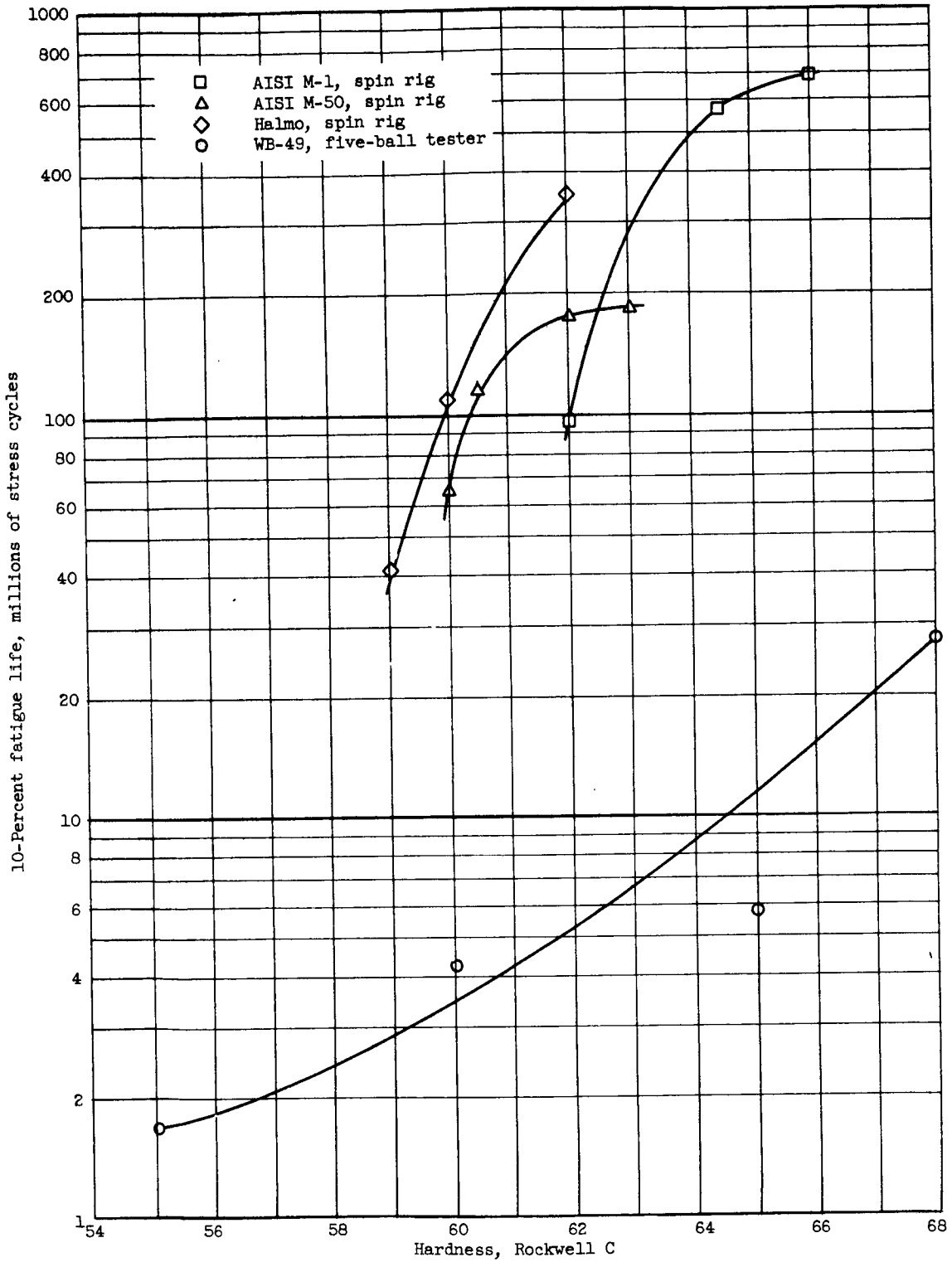


Figure 7. - 10-Percent fatigue failure life as a function of hardness for four alloy steels.

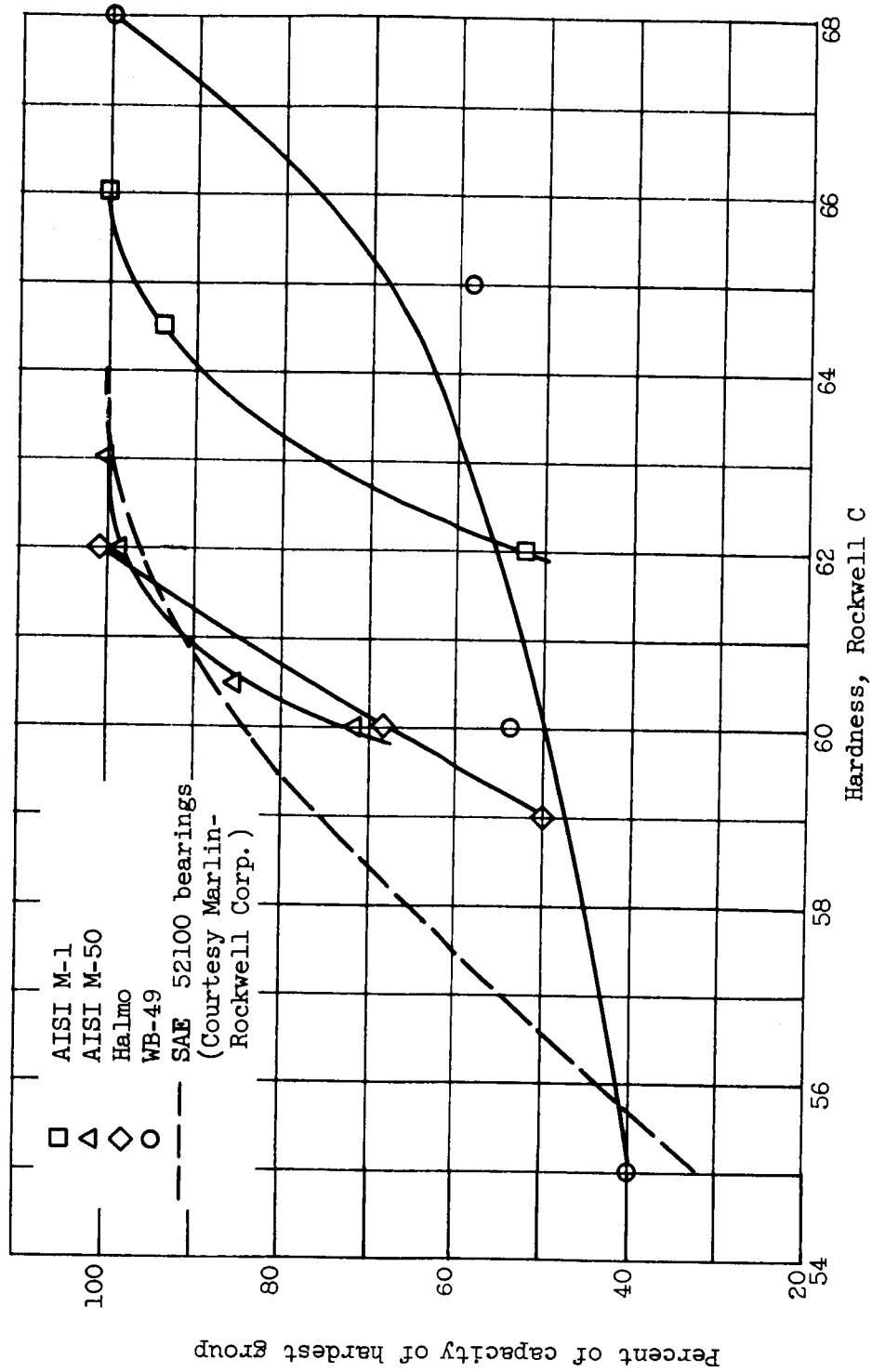


Figure 8. - Relative load-carrying capacity of bearing-steel balls tempered to different hardnesses.

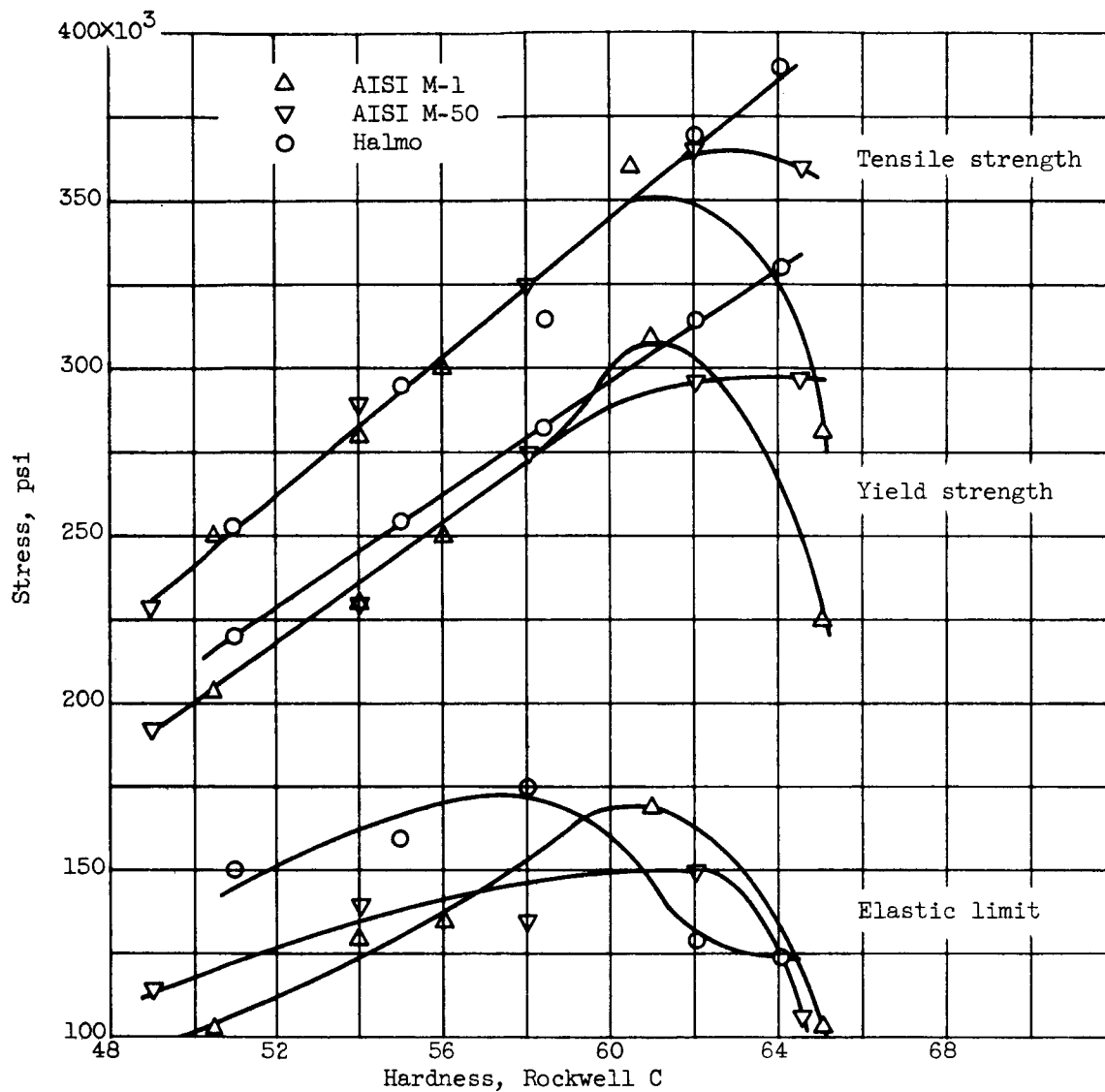
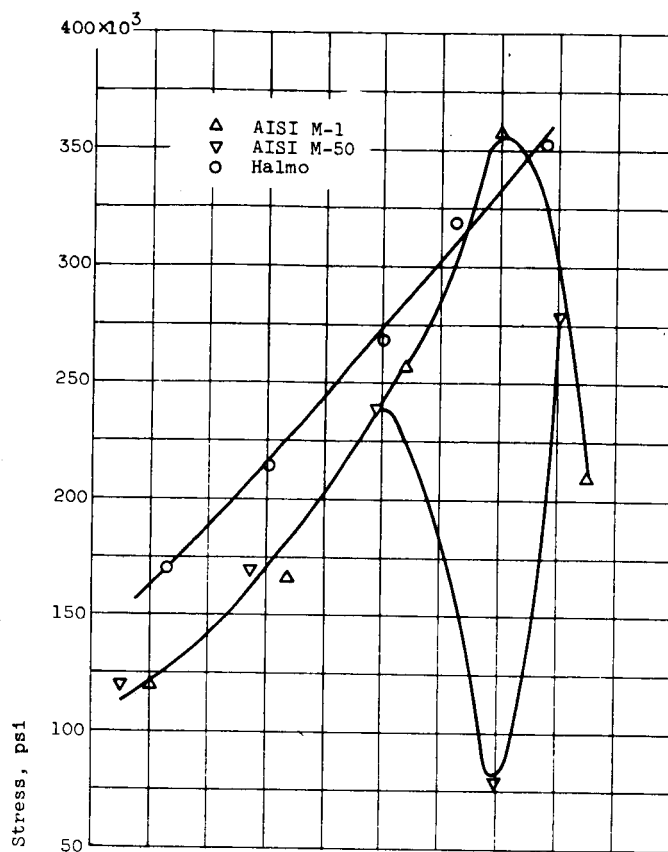
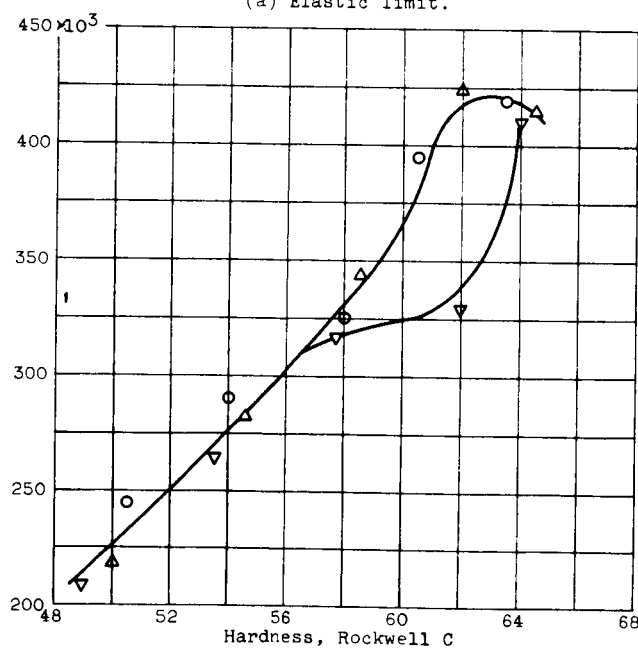


Figure 9. - Tensile properties of three tool steels tempered to various hardnesses (data from refs. 5 and 6).



(a) Elastic limit.



(b) Yield strength.

Figure 10. - Compressive properties of three tool steels tempered to various hardnesses (data from refs. 5 and 6).

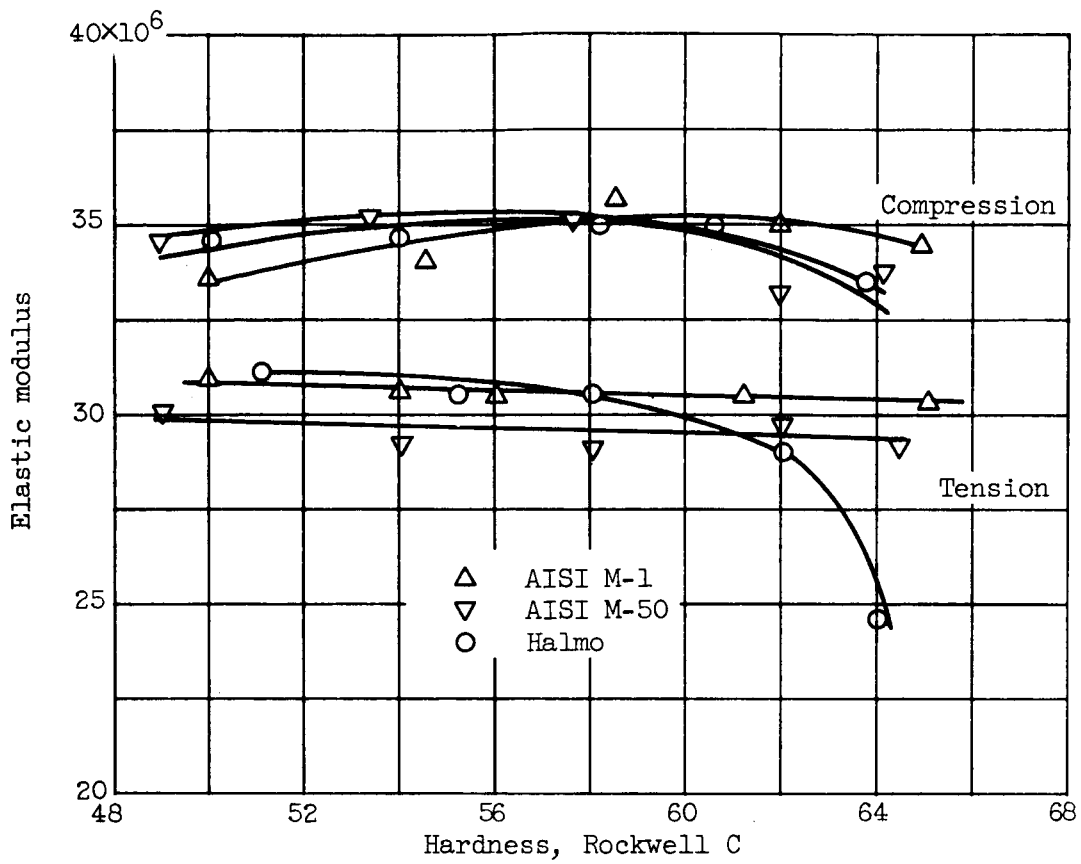


Figure 11. - Elastic modulus of three tool steels tempered to various hardnesses (data from ref. 6).

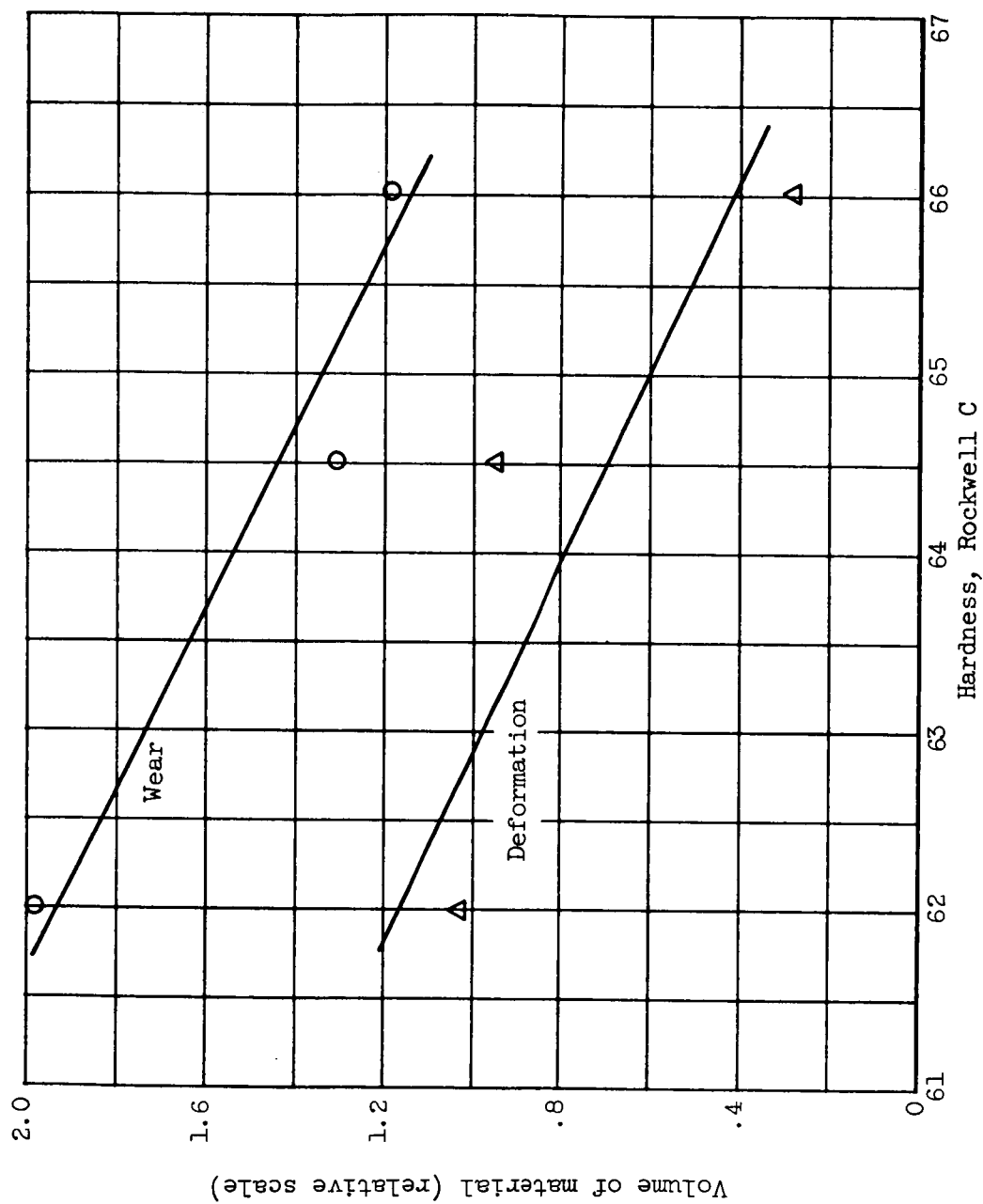


Figure 12. - Deformation and wear of AISI M-1 tool-steel-ball running tracks of varying hardness. Maximum Hertz compressive stress, 800,000 psi; 0° contact angle; 1.7×10^9 stress cycles; spin rig.

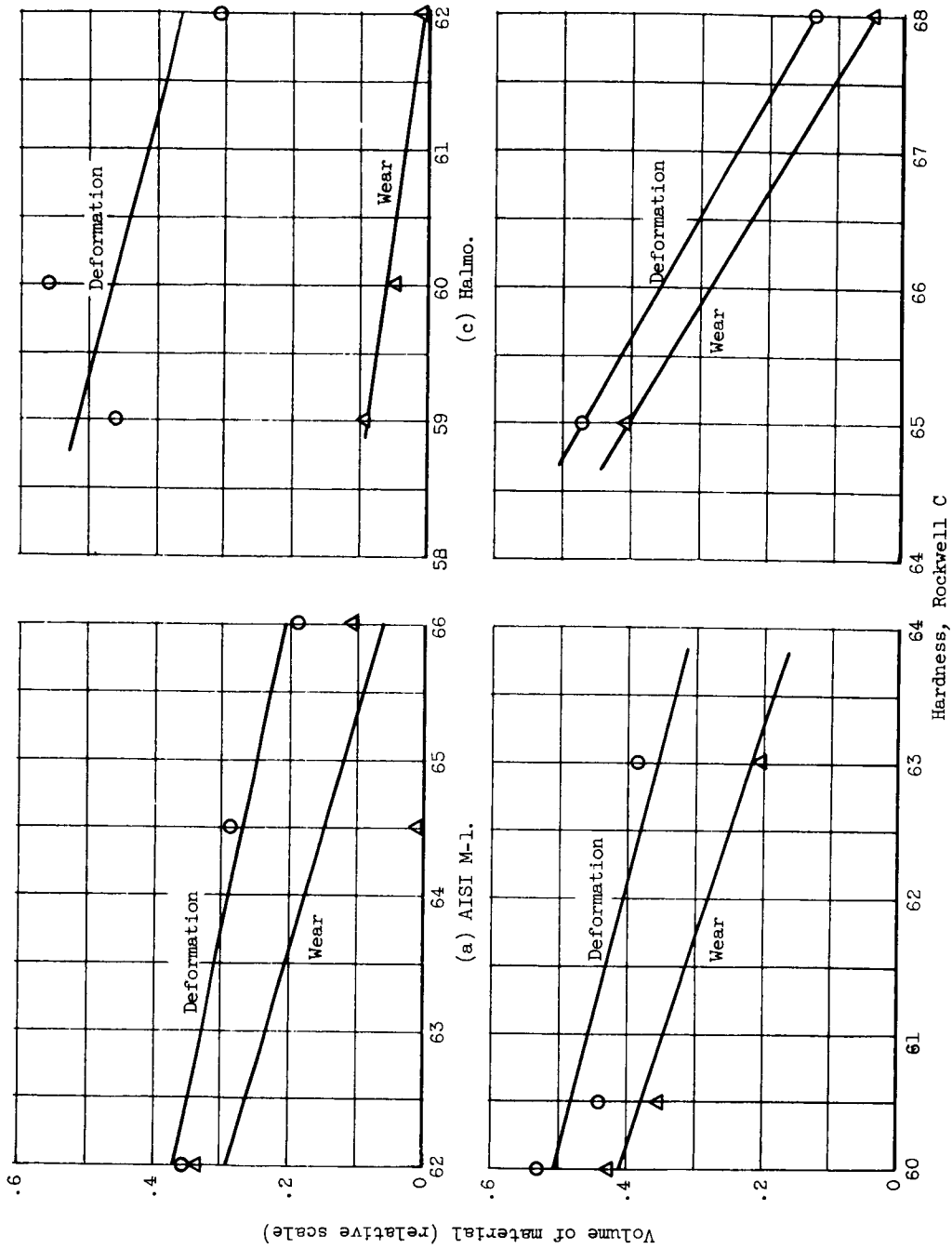
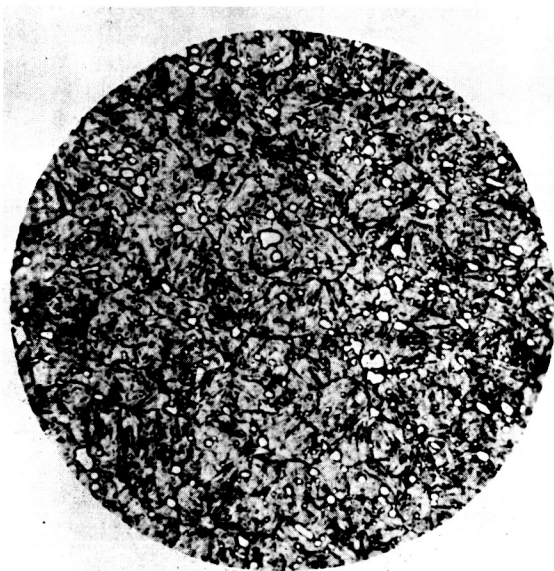
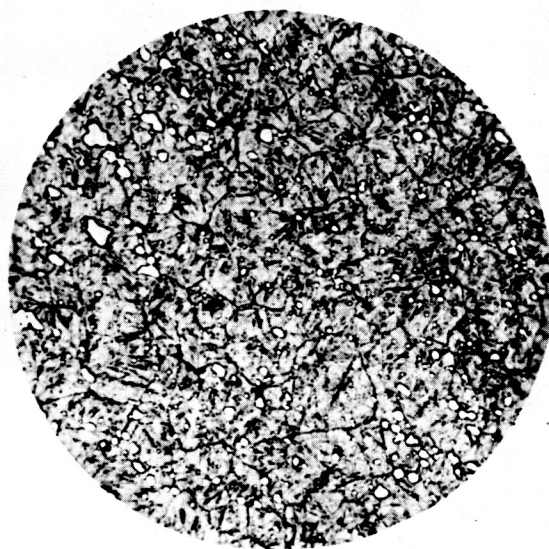


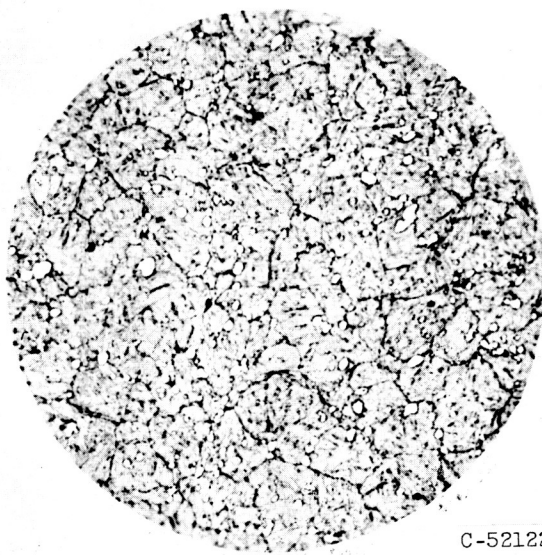
Figure 13. - Deformation and wear of tool-steel-ball running tracks of varying hardness.
Maximum Hertz compressive stress, 750,000 psi; 40° contact angle; 10,000 stress cycles;
five-ball tester.



(a) Rockwell C-62, double temper
2 hours at 1100° F.



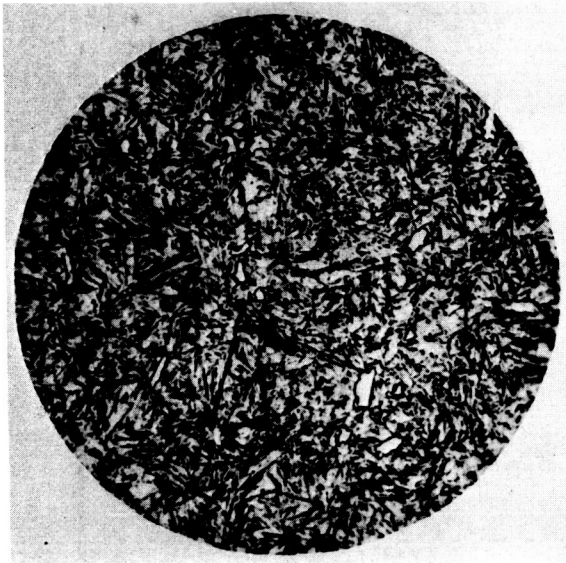
(b) Rockwell C-64.5, double temper
2 hours at 1050° F.



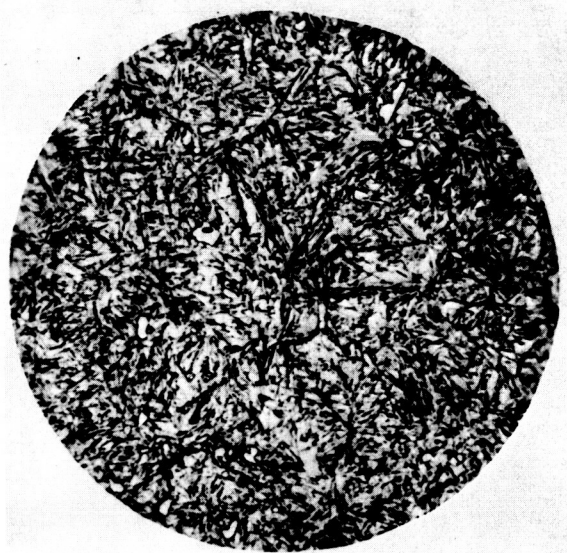
C-52122

(c) Rockwell C-66, double temper
2 hours at 1000° F.

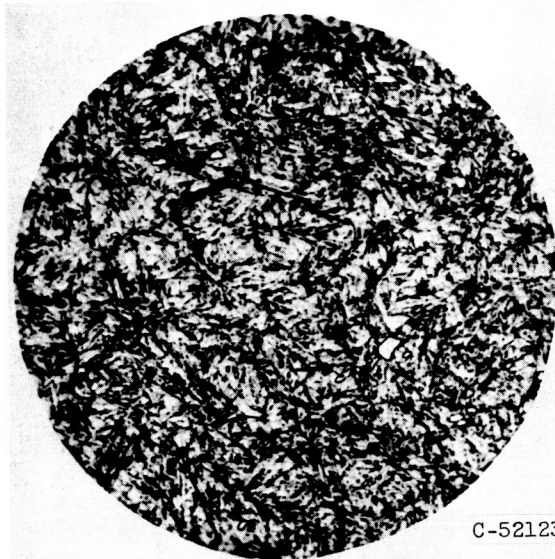
Figure 14. - Microstructure of AISI M-1 tool steel austenitized at 2200° F, oil quenched, and tempered as indicated. X750, figure reduced 20 percent in printing.



(a) Rockwell C-60, double temper
2 hours at 1100° F.

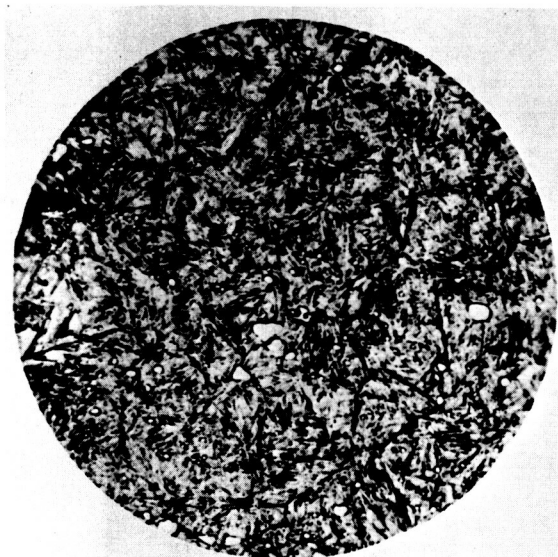


(b) Rockwell C-60.5, double temper
2 hours at 1050° F.

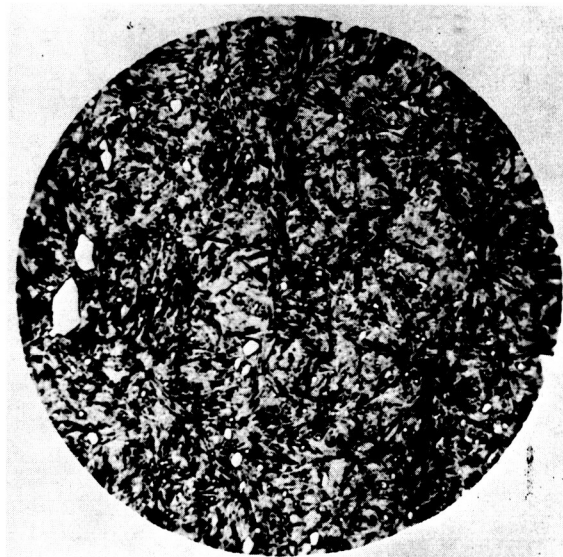


(c) Rockwell C-63, double temper
2 hours at 1000° F.

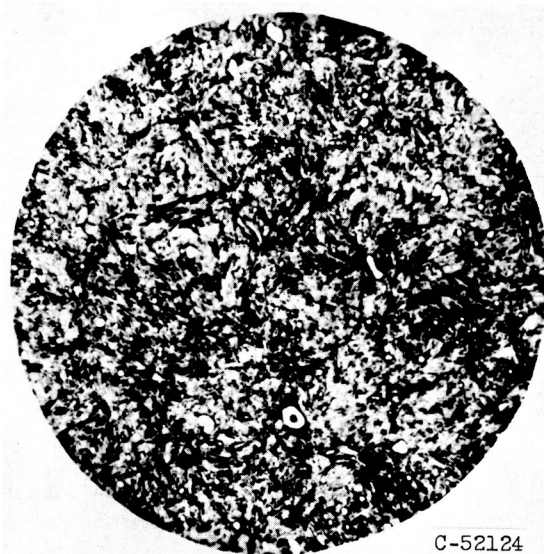
Figure 15. - Microstructure of AISI M-50 tool steel austenitized at 2050° F, oil quenched, and tempered as indicated. X750, figure reduced 20 percent in printing.



(a) Rockwell C-59, double temper
2 hours at 1100° F.

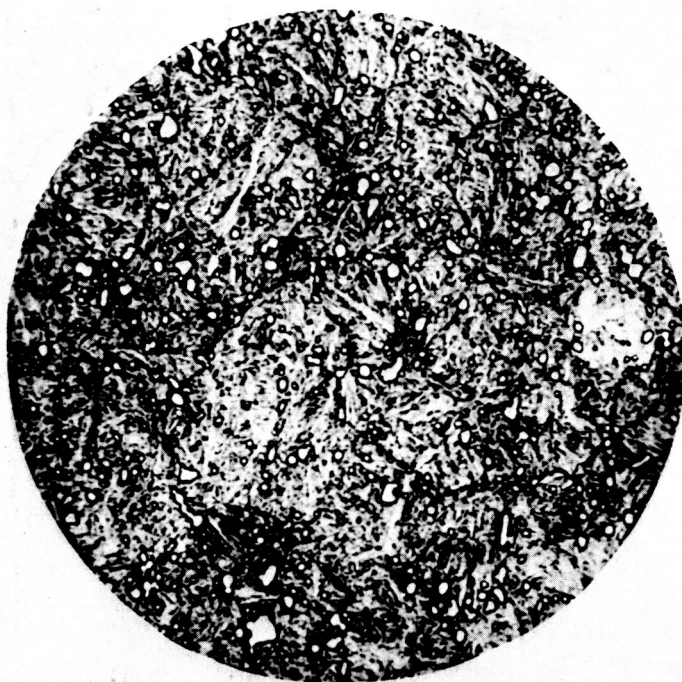


(b) Rockwell C-60, double temper
2 hours at 1050° F.

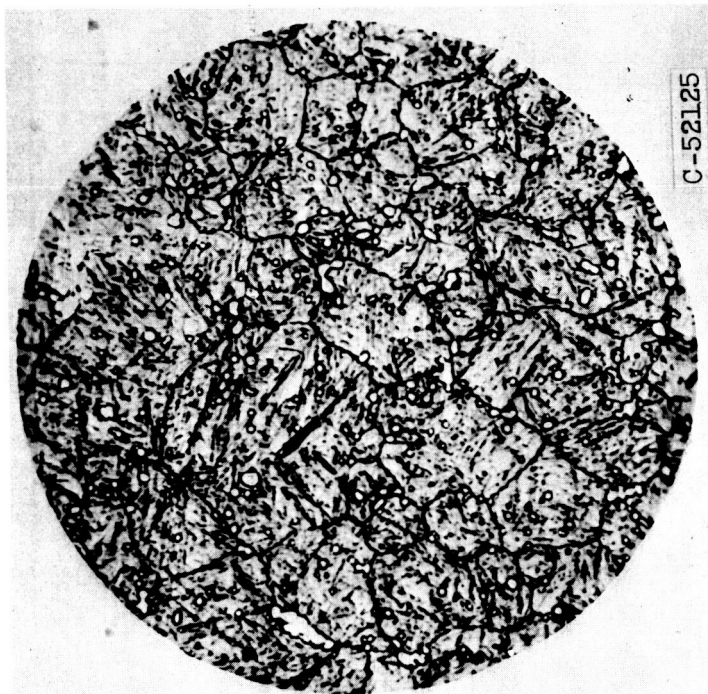


(c) Rockwell C-62, double temper
2 hours at 1000° F.

Figure 16. - Microstructure of Halmo tool steel austenitized at 2100° F, oil quenched, and tempered as indicated. X750, figure reduced 20 percent in printing.



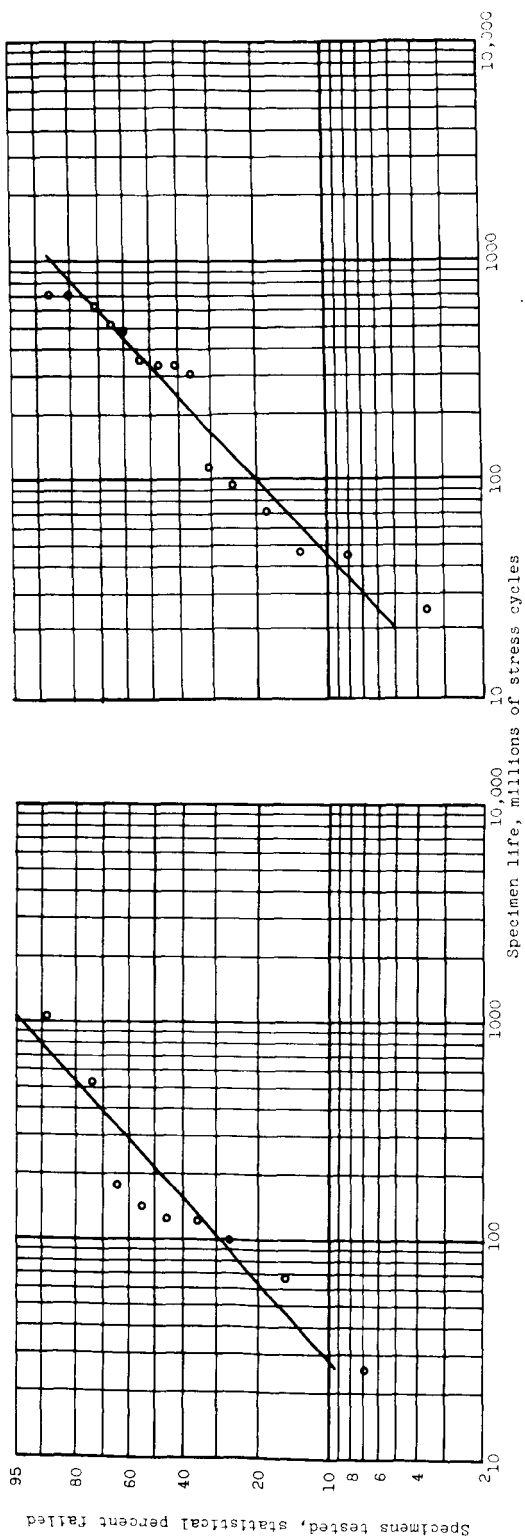
(a) Rockwell C-55, double temper
2 hours at 1025° F, third temper
40 minutes at 1250° F.



(b) Rockwell C-68, double temper
2 hours at 1025° F.

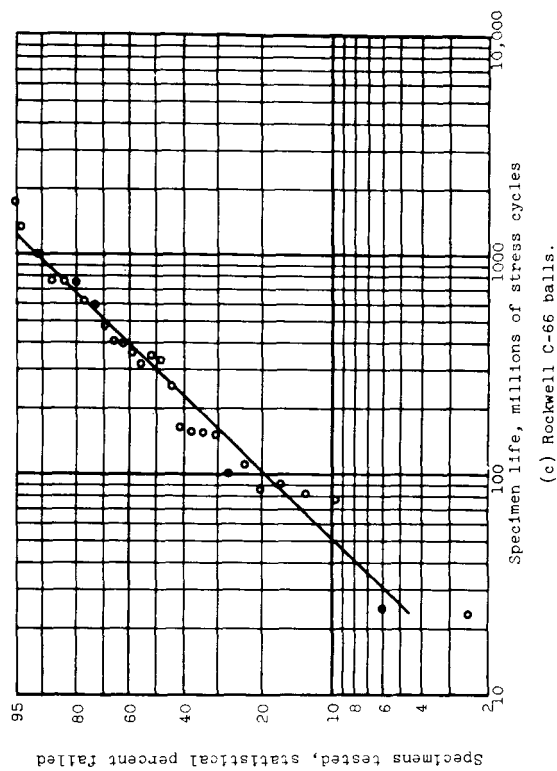
Figure 17. - Microstructure of WB-49 tool steel austenitized at 2225° F,
salt quenched to 1225° F for 6 minutes and cooled, and tempered as
indicated. X750.

E-524



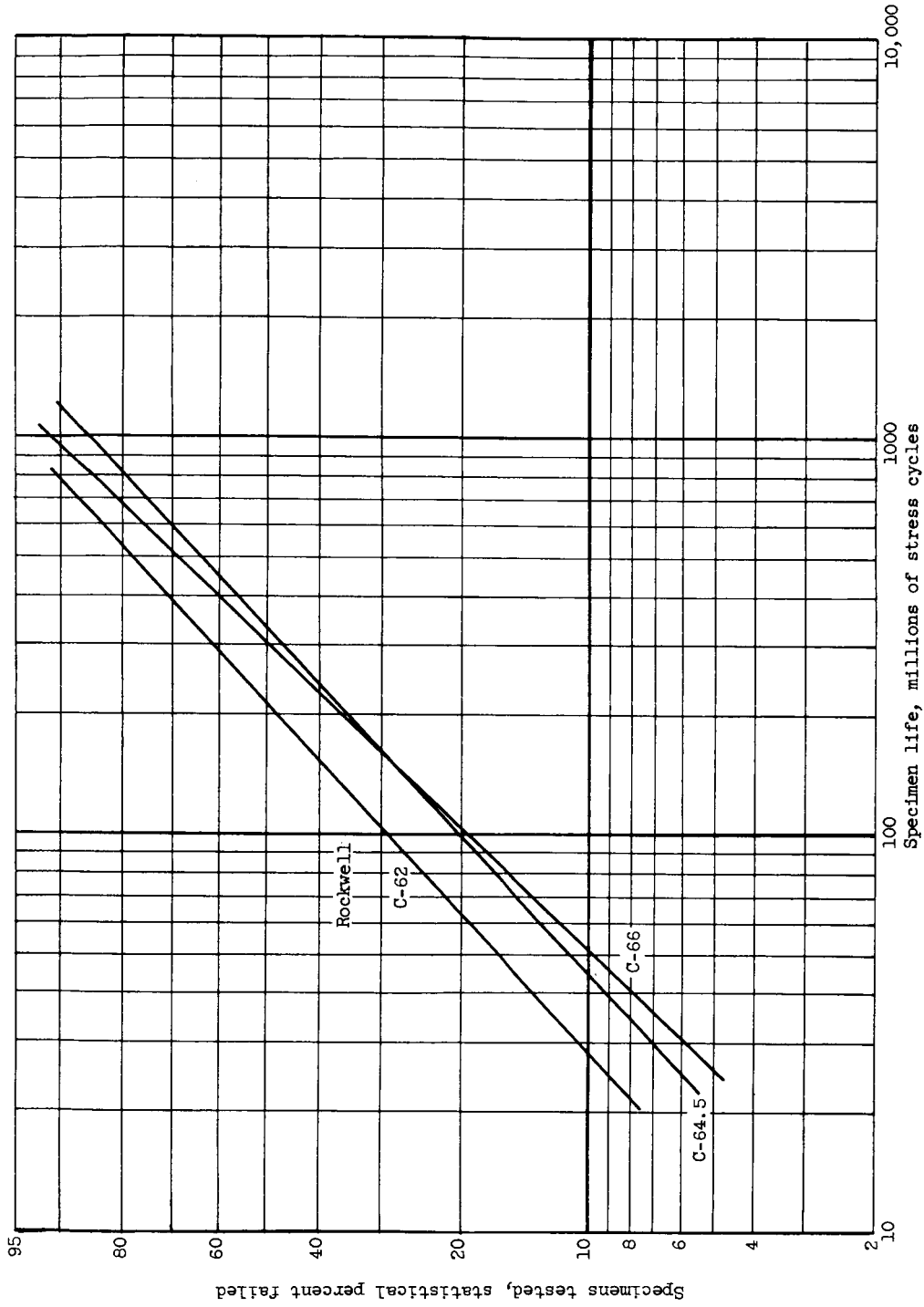
(a) Rockwell C-62 balls.

(b) Rockwell C-64.5 balls.



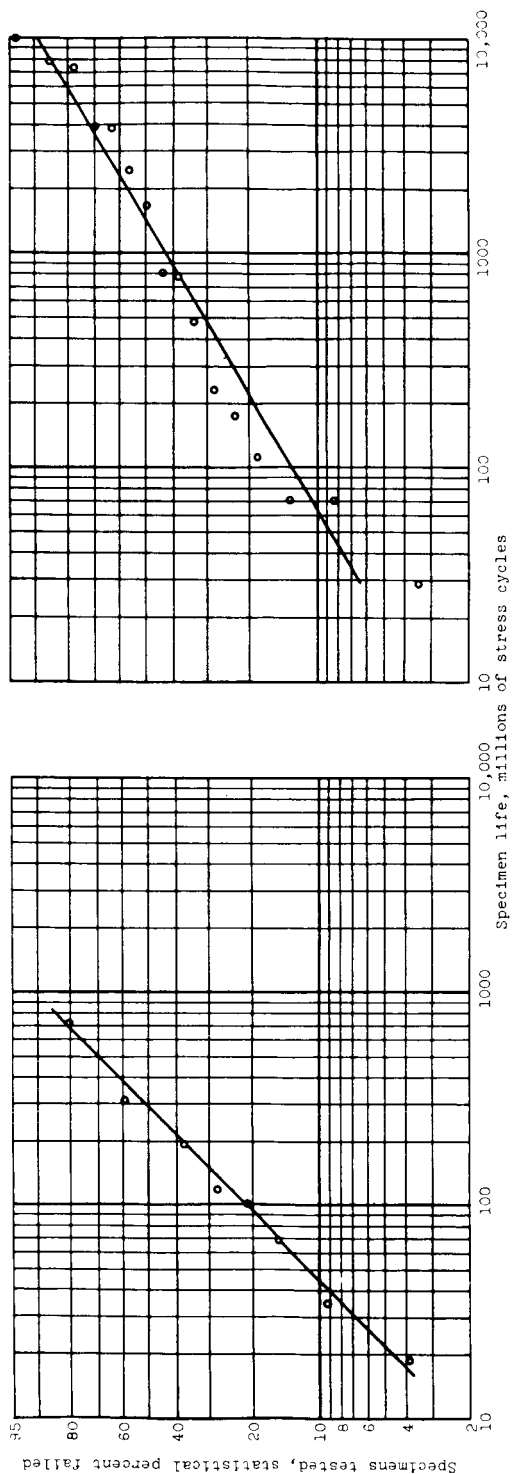
(c) Rockwell C-66 balls.

Figure 18. - Rolling-contact fatigue life of AISI M-1 tool-steel races (hardness, Rockwell C-62 to 63) run with M-1 balls of varying hardness. Maximum Hertz compressive stress, 800,000 psi; room temperature.



(d) Summary of race fatigue lives with balls of different hardness.

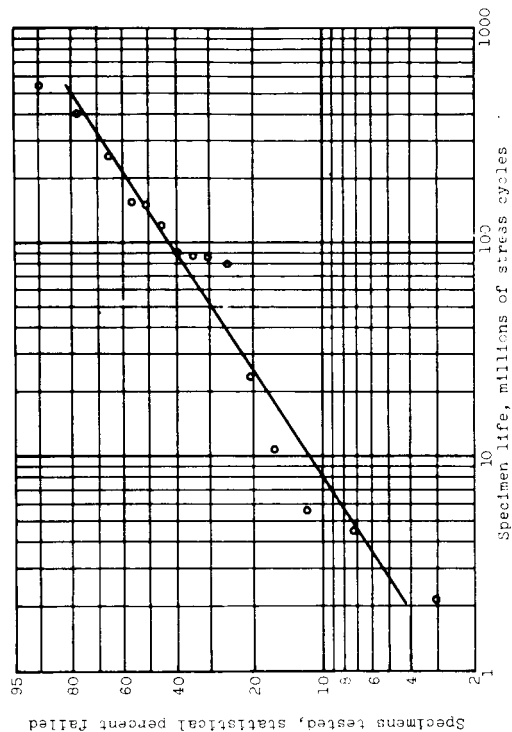
Figure 18. - Concluded. Rolling-contact fatigue life of AISI M-1 tool-steel races (hardness, Rockwell C-62 to 63) run with M-1 balls of varying hardness. Maximum Hertz compressive stress, 800,000 psi; room temperature.



(a) Rockwell C-60.

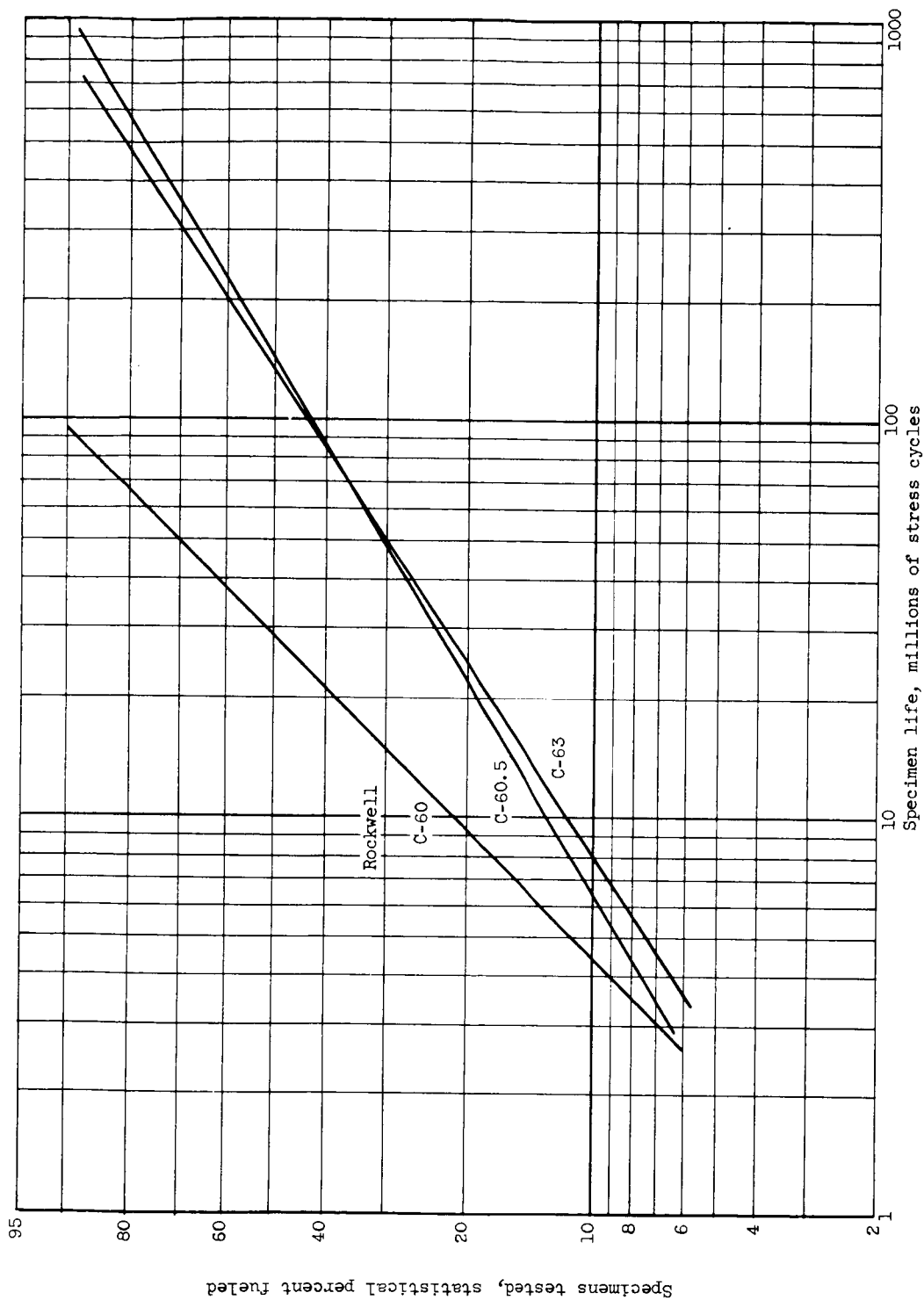


(b) Rockwell C-60.5.



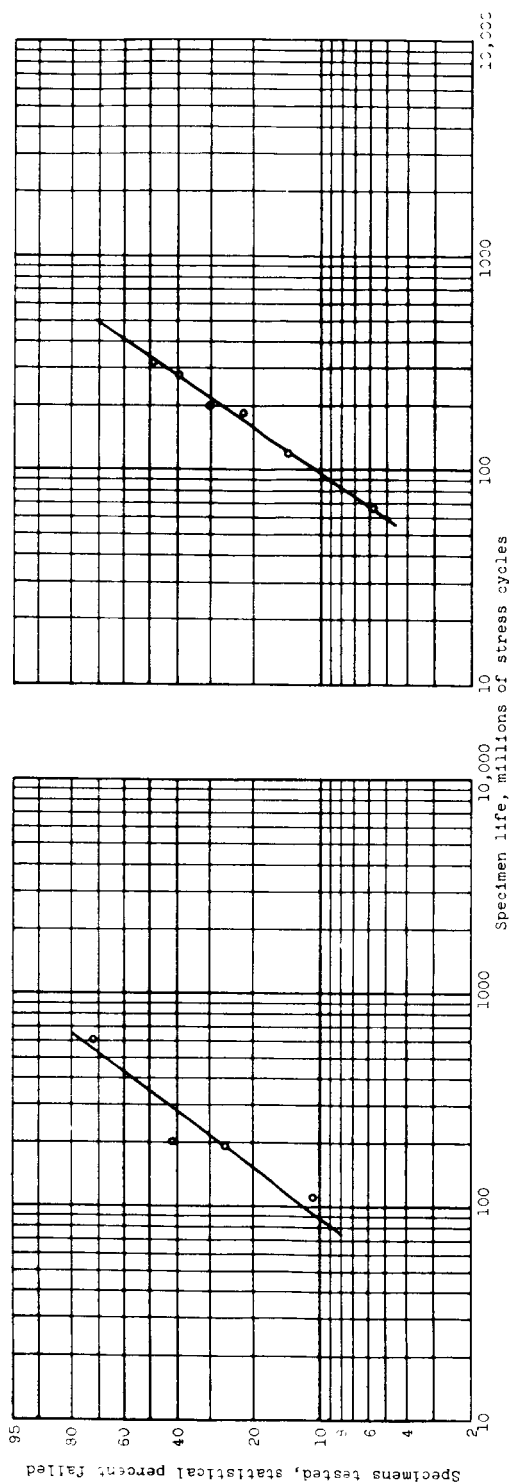
(c) Rockwell C-63.

Figure 19. - Rolling-contact fatigue life of AISI M-50 tool-steel races (hardness, Rockwell C-62 to 63) run with M-50 balls of varying hardness. Maximum Hertz compressive stress, 800,000 psi; room temperature.



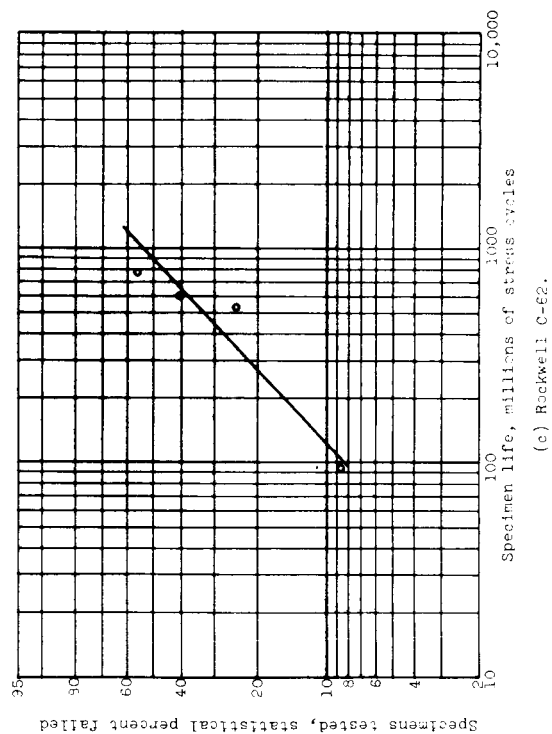
(d) Summary of race fatigue lives with balls of different hardness.

Figure 19. - Concluded. Rolling-contact fatigue life of AISI M-50 tool-steel races (hardness, Rockwell C-62 to 63) run with M-50 balls of varying hardness. Maximum Hertz compressive stress, 800,000 psi; room temperature.



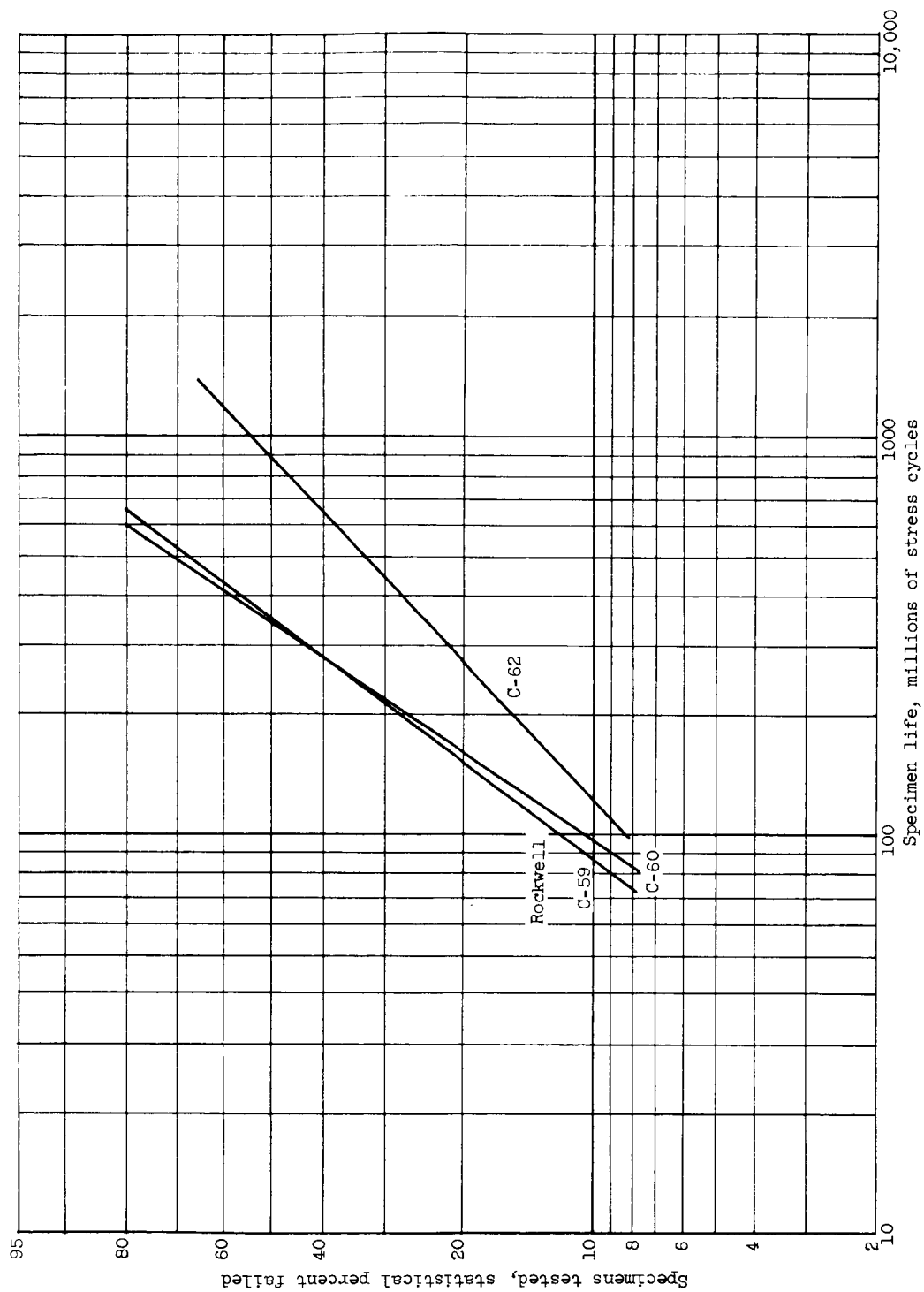
(a) Rockwell C-59.

(b) Rockwell C-60.



(c) Rockwell C-62.

Figure 20. - Rolling-contact fatigue life of Halmo tool-steel races (hardness, Rockwell C-62 to 63) run with Halmo balls of varying hardness. Maximum Hertz compressive stress, 750,000 psi; room temperature.



(d) Summary of race fatigue lives with balls of different hardness.

Figure 20. - Concluded. Rolling-contact fatigue life of Halmo tool-steel races (hardness, Rockwell C-62 to 63) run with Halmo balls of varying hardness. Maximum Hertz compressive stress, 750,000 psi; room temperature.